communications medicine

A Nature Portfolio journal

Article

https://doi.org/10.1038/s43856-025-00789-8

H105A peptide eye drops promote photoreceptor survival in murine and human models of retinal degeneration

Alexandra Bernardo-Colón[1], Andrea Bighinati[2], Shama Parween[3], Subrata Debnath[1], Ilaria Piano[4], Elisa Adani[2], Francesca Corsi[4], Claudia Gargini[4], Natalia Vergara[3,5], Valeria Marigo[2,6] ✉ & S. Patricia Becerra[1,6] ✉

Abstract

Background Photoreceptor death leads to inherited blinding retinal diseases, such as retinitis pigmentosa (RP). As disease progression often outpaces therapeutic advances, developing effective treatments is urgent. This study evaluates the efficacy of small peptides derived from pigment epithelium-derived factor (PEDF), which are known to restrict common cell death pathways associated with retinal diseases.

Methods We tested chemically synthesized peptides (17-mer and H105A) with affinity for the PEDF receptor, PEDF-R, delivered as eye drops to two RP mouse models: *rd10* (phosphodiesterase 6b mutation) and $Rho^{P23H/+}$ (rhodopsin P23H mutation). Additionally, we engineered AAV-H105A vectors for intravitreal delivery in $Rho^{P23H/+}$ mice. To assess peptide effects in human tissue, we used retinal organoids exposed to cigarette smoke extract, a model of oxidative stress. Photoreceptor survival, morphology and function were evaluated.

Results Here we show that peptides 17-mer and H105A delivered via eye drops successfully reach the retina, promote photoreceptor survival, and improve retinal function in both RP mouse models. Intravitreal delivery of a AAV-H105A vector delays photoreceptor degeneration in $Rho^{P23H/+}$ mice up to six months. In human retinal organoids, peptide H105A specifically prevents photoreceptor death induced by oxidative stress, a contributing factor to RP progression.

Conclusions PEDF peptide-based eye drops offer a promising, minimally invasive therapy to prevent photoreceptor degeneration in retinal disorders, with a favorable safety profile.

Plain language summary

Retinitis pigmentosa (RP) is a rare inherited condition that causes the gradual death of photoreceptors (light-sensing cells) in the eye, leading to vision loss. There is currently no cure. This study tested a potential treatment using small protein fragments (peptides) from PEDF, a protective protein naturally found in the eye. Researchers delivered these peptides through eye drops or gene therapy in mouse models of RP and to human retinal organoids (lab-grown retina tissue). Mice treated early maintained healthy vision cells, while untreated mice experienced rapid cell loss and vision decline. These results suggest that peptide-based eye drops could be a simple, safe, and effective way to slow vision loss in patients with RP.

Retinal degenerative diseases, such as inherited retinal dystrophies (IRDs), and age-related macular degeneration (AMD) are major causes of untreatable blindness. Retinitis pigmentosa (RP), the most common group of IRDs, is characterized by progressive photoreceptor cell loss that leads to blindness[1,2]. Although RP is a relatively rare genetic disorder, it is estimated to affect 1 in 4000 people worldwide[3]. Its prevalence varies significantly depending on the population studied and the mutations involved in each RP type. Because the known RP genetic heterogeneity makes developing RP therapeutics rather challenging, gene-independent approaches (e.g., neuroprotective agents, retinal implants, gene therapy, dietary supplements, low-vision aids, and rehabilitation) aiming to treat a wider patient population have become more appealing[2,4–8]. Moreover, most ocular drug delivery routes for effective and specific targeting of photoreceptors (e.g., intravitreal or subretinal injections, intracameral injections using nanoparticles, liposome implants, intravenous administration, and others) involve various degrees of invasiveness[9–11]. Importantly, as RP has a

[1]Section of Protein Structure and Function, Laboratory of Retinal Cell and Molecular Biology, National Eye Institute, National Institutes of Health, Bethesda, MD, USA. [2]Department of Life Sciences, University of Modena and Reggio Emilia, 41125 Modena, Italy. [3]CellSight Ocular Stem Cell and Regeneration Program, Sue Anschutz-Rodgers Eye Center, University of Colorado Anschutz Medical Campus; Aurora, Colorado, USA. [4]Department of Pharmacy, University of Pisa, 56126 Pisa, Italy. [5]Gates Center for Regenerative Medicine, Linda Crnic Institute for Down Syndrome and University of Colorado Alzheimer's and Cognition Center, University of Colorado Anschutz Medical Campus, Aurora, CO, USA. [6]These authors contributed equally: Valeria Marigo, S. Patricia Becerra.
✉e-mail: vmarigo@unimore.it; becerras@nei.nih.gov

substantial impact on affected patients, finding potential RP treatments and identifying interventions to improve their quality of life are urgent clinical needs.

Current RP mouse models involve animals spontaneously mutated, or genetically engineered, replicating RP-associated genetic mutations in humans. Here, we selected two well-characterized models, *rd10* and *Rho*$^{P23H/+}$ mice, that represent different genetic forms of RP with different rates of disease progression yet share photoreceptor cell death mechanisms. The *rd10* mouse is a model of autosomal recessive RP and has a spontaneous mutation in the *Pde6b* gene that inactivates phosphodiesterase PDE6, an enzyme involved in visual phototransduction[12]. This mutation, also present in ~5% human RP patients, leads to photoreceptor degeneration and simulates the disease process in humans[1,12–15]. We also used the *rd10/Serpinf1*$^{-/-}$mouse model, in which the deficiency of *Serpinf1* (the gene encoding pigment epithelium-derived factor (PEDF) protein) increases susceptibility to retinal degeneration[16]. The Pro23His (P23H) variant is the most frequent mutation in the rhodopsin (*RHO*)-encoding gene, and alone accounts for ~10% of autosomal dominant RP cases in North America. *Rho*$^{P23H/+}$ mice carry the P23H mutation engineered into the *Rho* gene and exhibit progressive retinal degeneration as in human patients[17]. While in the *rd10* mouse photoreceptor death is completed in one month after birth, the photoreceptor degeneration in the *Rho*$^{P23H/+}$ mouse progresses much slower and most photoreceptors are absent by 180 days of age. Despite the different mutations, the mechanism of photoreceptor cell death in these two RP mutant retinas is associated with the calcium-calpain pathway. In the calcium-calpain pathway, an overload of intracellular calcium triggers calpain proteases, which then act on apoptosis-inducing factor through BAX activation[18]. Furthermore, photoreceptor loss in RP models is also linked to oxidative stress[18]. Thus, we used human-induced pluripotent stem cell (iPSC)-derived retinal organoids (ROs) subjected to oxidative stress-induced damage, as they replicate key features of retinal degeneration observed in RP[19–21].

The PEDF protein is known to prevent retinal degenerative processes by interfering with photoreceptor cell death pathways, is not toxic to humans or mice, and consequently holds promise as a useful RP therapeutic agent[22–25]. One of the key benefits of PEDF is that its protective effects on photoreceptors are independent of the specific gene mutation causing the degeneration, thus offering a broad-spectrum approach to therapy. We have previously shown that PEDF activates the phospholipase activity of its receptor, PEDF-R, on retinal cells, which is crucial for its neurotrophic effects[26,27]. Notably, ablation of PEDF-R leads to photoreceptor degeneration in mice, underscoring the importance of this pathway[28]. In an effort to harness these protective effects, we have designed neuroprotective peptides from PEDF, namely 17-mer and its variant H105A, which target PEDF-R and are involved in mitigating calcium overload in degenerating photoreceptors associated with RP[29–33]. These short PEDF-derived peptides have potential benefits in neuroprotection[22,23,29–33], a key feature that makes them promising candidates for further research.

The delivery method of these peptides is a critical factor for their efficacy. This study explores whether administering PEDF peptides via eye drops - an understudied delivery method for targeting photoreceptors - could effectively deliver these peptides to the retina. The goal is to determine whether these delivery methods can delay, stabilize, or prevent progression of IRDs such as RP. To address these questions, our research investigates the survival effects of PEDF peptides on photoreceptors using preclinical mouse models of RP. Additionally, we explore an alternative delivery method involving gene therapy vectors (currently FDA-approved for other indications) as well as testing in human ROs. We demonstrate that peptides 17-mer and H105A, administered via eye drops, successfully reach the retina, promote photoreceptor survival, and enhance retinal function in both RP mouse models. Additionally, intravitreal delivery of a AAV-H105A vector delays photoreceptor degeneration in *Rho*$^{P23H/+}$ mice for up to six months. In human retinal organoids, peptide H105A specifically protects photoreceptors from oxidative stress-induced cell death, a key factor in RP progression. These models provide a framework for evaluating the therapeutic potential and feasibility of PEDF peptide delivery methods, paving the way for future translational research and clinical applications in RP treatment.

Methods

Animals

Experimental animals *rd10* mice ($n = 50$) (from Jackson Laboratories), *rd10/Serpinf1*$^{-/-}$ ($n = 50$) (*rd10* mice crossed with *Serpinf1 null* mice, double mutant mice[16]) and C57BL/6 J ($n = 15$) (from Jackson Laboratories) of P0-P25 days old were maintained in the animal facility of the National Institutes of Health, USA. Experimental animals *Rho*$^{P23H/+}$[17] ($n = 51$) from P0 to P180 were maintained in the animal facility CSSI (Centro Servizi Stabulario Interdipartimentale, Italy). All animals were bred in the C57BL/6 J background, on normal chow diet and a 12 h light/dark cycle. All the experimental procedures were approved by the National Eye Institute Animal Care and Use Committee and the Ethical Committee of University of Modena and Reggio Emilia and by the Italian Ministero della Salute (150/2021-PR) and were performed as per guidelines of the Association for Research in Vision and Ophthalmology statement for the Use of Animals in Ophthalmic and Vision Research and in accordance with the ARRIVE guidelines.

We did not select either males or females in our studies because the murine models here used have not been reported to show differences in the progression of the disease between sexes, as also reported in patients with mutations in the PDE6 enzyme or P23H mutation in rhodopsin. Therefore, based on the "reduction" 3 R requirement for animal studies, we did not exclude animals from the study, and all the bred animals participated in the study. For the experiments, the ages of the mice were between P15 and P25 for *rd10*, and P5 and P180 for *Rho*$^{P23H/+}$, with both males and females included in the experiments.

Peptides and proteins

We designed peptides from PEDF, namely 17-mer and its variants H105A and R99A (Fig. 1a). These peptides were chemically synthesized and purified to ≥95% purity (Biosynthesis Inc. and LifeTein). They were conjugated to Alexa Fluor 488 dye to produce fluorescently labeled peptides (BioSynthesis, and LifeTein). The peptide sequences used in the study are shown in Supplementary Table 1.

Lyophilized peptides were dissolved in sterile HBSS at 1 mg/ml and stored at −20 °C. Before the peptides were used, the peptide solution was brought to room temperature and subjected to centrifugation (Eppendorf, Centrifuge 5430 R) at 20,800 x *g* for 10 min at 4 °C to clear and separate particulate material. In case a precipitate was found, the pH of the solution was adjusted to neutral pH with either NaOH or HCl and all peptides were soluble. The concentration of peptide solutions was determined using spectrophotometry (NanoDrop, Thermo Fisher Scientific). The stability of peptide H105A against temperature was performed and summarized in Supplementary Table 2.

To obtain the PEDF-R protein, the following procedure was followed. For plasmid construction, the plasmid used for expression was pE-SUMOstar-PEDF-R[1–288] C-terminal TwinStrep tagged. This plasmid contained the coding sequence for the human PEDF-R open reading frame between positions 1 and 288. For transformation: The expression plasmid and pGro7(groES-groEL) were co-transformed into *Escherichia coli* Rosetta(DE3) to obtain colonies for recombinant protein expression[34,35]. The transformed cells were plated on Luria-Bertani (LB) agar plate containing 10 μg/ml chloramphenicol and 100 μg/ml ampicillin followed by overnight incubation at 37 °C to obtain colonies. A total of 100 ml of LB media containing 10 μg/ml chloramphenicol and 100 μg/ml ampicillin was inoculated with a single colony and incubated at 37 °C with vigorous shaking overnight. Then, 1 liter of LB media containing 0.5 mg/ml L-(+) arabinose, 2% D-(+)-Glucose, 10 μg/ml chloramphenicol and 100 μg/ml ampicillin was inoculated with 2% of the overnight culture and incubated at 37 °C with vigorous shaking until the $O.D._{600\ nm}$ reached 0.5-0.6. Proteins expression was induced by addition of 0.5 mM isopropyl-β-D-thiogalactopyranoside (IPTG) at 25 °C for overnight. For cell harvesting:

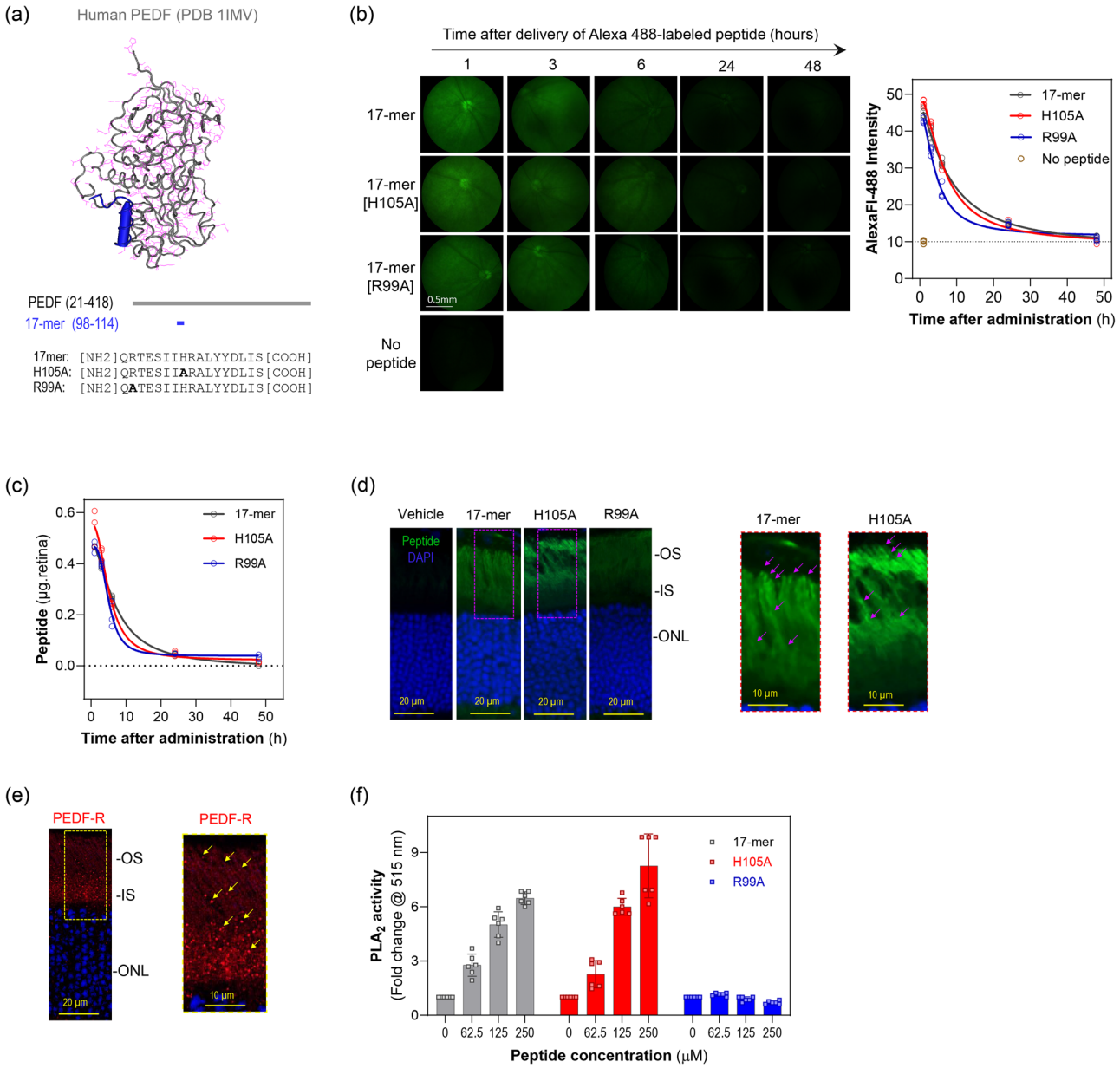

Fig. 1 | Penetration and bioavailability of PEDF Peptides 17-mer, H105A, and R99A Delivered via Eye Drops in Mouse Retinas. a Peptide mapping and sequence. Tertiary structure of human PEDF highlighting the small peptide region with neurotrophic activity (17-mer) in blue (top). Primary structure of human PEDF showing the location of the 17-mer region (middle). Sequences of the 17-mer peptide and its variants, H105A and R99A (bottom). **b** In vivo detection of peptides. Fundus micrographs showing fluorescence from Alexa Fluor 488-labeled 17-mer, H105A, and R99A peptides in the eyes of C57BL/6J mice at P21 days after eye drop administration of 5 µl of peptide at 1 mg/ml (left). Fundus images were taken at 1, 3-, 6-, 24-, and 48 h post-administration. Quantification of fluorescence intensity over time post-administration (right). The plot shows average intensity from three regions of interest (R.O.I.s) per eye, with five eyes ($n = 5$) per time point. **c** Quantification of peptide in retinas. The plot shows the amounts of AlexaFluor-488-labeled peptides (17-mer, H105A, R99A) detected in dissected retinas at each time point. The amount of peptide was quantified from the fluorescence in retinal extracts using standard curves (Supplementary Fig. 1a). Each data point represents the amount of each peptide per eye with three eyes (n = 3) per time point. **d** Retinal cross-sections showing fluorescence distribution in the photoreceptor layer 1 h after applying eye drops as in Panel B. Representative images for labeled 17-mer, H105A, and R99A peptides are shown, with magnified areas of 17-mer and H105A indicated by dotted rectangles. Magenta arrows point to punctuated areas in the outer segments (OS). IS, inner segments; ONL, outer nuclear layer. **e** Retinal sections showing PEDF-R distribution (red) and DAPI (blue) in C57BL/6 J mice at P21. Three retinas ($n = 3$) were used per group, with a representative image shown. A magnified area (yellow dotted rectangle) is provided. **f** Effects of 17-mer, H105A, and R99A peptides on the PLA_2 activity of PEDF-R. Peptides were preincubated with recombinant human PEDF-R[1–288] for 30 min, and PLA_2 activity was measured. Each bar represents the average fold-change in activity over control (no peptide) (mean ± SD), from six replicate enzymatic reactions with indicated peptide concentrations and final concentration for PEDF-R of 60 nM.

Cells were grown to the desired density and then harvested by centrifugation. For cell lysis: The harvested cells were resuspended in buffer A (50 mM Tris-HCl, pH 8.0, 500 mM NaCl, 20% Glycerol, 1 mM tris(2-carboxyethyl) phosphine (TCEP), 0.1% IGEPAL CA-630, 0.5% (W/V) 3-[(3-cholamidopropyl)dimethylammonio]-1-propanesulfonate (CHAPS) and 10 mM Imidazole) containing EDTA-free protease inhibitor cocktail. The cells were then lysed, and the lysates were cleared by centrifugation at 33,745 x *g* for 30 min at 4 °C. For affinity chromatography: The supernatant with the cleared lysate was subjected to two-step affinity column chromatography using a HisTrap HP column followed by a StrepTrap XT column. This

process was performed using an automated ÄKTA pure™ chromatography system (Cytiva). Fractions containing the recombinant protein were collected and pooled. The pooled fractions were concentrated, resulting in a recombinant PEDF-R[1–288] protein that was >90% pure, soluble, and active. This protocol ensured the successful purification of the recombinant PEDF-R protein, which was used for further experiments and analyses.

Retinal extracts

Protein extracts were obtained from dissected mouse retinas in RIPA Lysis and Extraction Buffer (Thermo Fisher Scientific, cat. 89900) containing protease inhibitors (Pierce Protease Inhibitor Tablets, Thermo Fisher Scientific, cat. A32963) at 80 µl per retina. The retinal tissues were disrupted using a Sonic Dismembrator (FisherBrand™ Model 50) set at 30 in the amplitude dial for 15 s in ice-water bath (at 4 °C), followed by centrifugation at 20,800 x *g* for 10 min at 4 °C to remove particulate material[28].

Eye drop administration

In a sterile hood, aliquots of the peptide solutions were prepared from the stocks. Administration to each mouse eye was with a volume of 5 µl at the indicated concentrations and regimen of treatment (see schemes in figures). The eye drops were administered by the same investigator throughout the study for consistency.

Quantification of peptides in the retina

Each Alexa Fluor-488 labeled peptide solution was administered via 5 µl of eye drops containing peptide at 1 mg/ml concentration per eye of wild type mice. At end point, retinal protein extracts were prepared from each enucleated eye. A total of 30 µl of each freshly prepared soluble retinal extract was added to a well in 96-well plate in triplicates. Fluorescence was determined using a fluorometer (POLARstar OPTIMA) using a wavelength at 485 nm for excitation and at 520 nm for emission. Retinal extract without peptide was used as a background control set at zero. The amount of peptide in the retina was determined from the fluorescence and using standard curves (Supplementary Fig. 1a).

Standard curves of Alexa Flour-488 labeled peptides

Retinal extracts from three C57BL/6 J mouse eyes were prepared, pooled and used to dilute the labeled peptides. Solutions of Alexa Flour-488 labeled-17-mer, -H105A and -R99A peptides at concentrations that ranged between 0.0 µg/ml and 0.0625 µg/ml were prepared in retinal extracts. A total volume of 30 µl of each was added to a well of a 96-well plate. The fluorescence in the retinal extract was determined with a plate reader of a fluorometer (POLARstar OPTIMA) using a wavelength at 485 nm for excitation and at 520 nm for emission. Plots were prepared from the fluorescence as a function of peptide concentration using GraphPad. Standard curves were used to quantify the labeled peptides 17-mer, H105A and R99A in the retina extracts. Alexa Flour-488 labeled peptides 17-mer and H105A exhibited neuroprotective activity, as assessed by ERG, indicating they were functional peptides, but R99A was not (Supplementary Fig. 1b).

Phospholipase A_2 activity assay

Phospholipase A_2 (PLA_2) activity was determined using EnzChek™ Phospholipase A2 Assay Kit (Thermo Fisher Scientific, cat. E10217) according to the manufacturer's instructions and as described before[28]. Protein samples (retinal extracts or PEDF-R[1–288], as described above) were mixed with peptides and preincubated at room temperature for 30 min and diluted up to 50 µl before enzymatic evaluation. Briefly, 50 µl of the sample were transferred to a microplate well (96-well plate). A lipid mixture was prepared by mixing 15 µl 10 mM dioleoylphosphatidylcholine (DOPC), 15 µl 10 mM dioleoylphosphatidylglycerol (DOPG) and 15 µl 1 mM PLA_2 substrate. Then, a substrate-liposome was prepared by mixing 25 µl lipid mixture with 2.5 ml 1X PLA_2 reaction buffer by stirring. A total of 50 µl of substrate-liposome mixture was added to each microplate well containing the sample and incubated at room temperature for 10 min, protected from light. The final reaction volume was 100 µl. Fluorescence emission was measured at 515 nm with excitation at 460 nm. The final concentration of PEDF-R[1–288] was 60 nM in the reaction mixture.

In vivo photoreceptor degeneration assessment in *rd10* and *rd10/Serpinf1*$^{-/-}$ murine models

Fluorescence fundoscopy with a cell death probe was chosen as a simple method for monitoring photoreceptor cell death in alive animals[36]. A fluorescent probe, bis (zinc^{2+}-dipicolylamine)-550, (PSVue®-550) (Molecular Targeting Technologies Inc, cat. P-1005) was reconstituted in Hanks' Balanced Salt Solution (HBSS, Quality Biological, cat. 114-062-101) according to the manufacturer's instructions[28,36]. This probe is suitable for in vivo use to specifically and transiently label dying photoreceptors, such as in living rats with retinal degeneration the Royal College of Surgeons rat model, in a non-invasive and non-toxic method without the need of intraocular injection[36]. Briefly, a stock of 1 mM solution of PSVue®-550 was stored in the dark at 4 °C and used within 14 days directly as eye drop. After 3-4 h of light onset each mouse received eye drops of 5–10 µl of 1 mM PSVue®-550 in the left eye and HBSS in the right eye as control. The eye drop volume was chosen such that the eye cavity was filled without spillage outside the eye, and it was modified depending on eye size. Eyes of mice that did not receive the probe were used as background controls. To obtain in vivo retinal images of fundi, at 24 h after the probe was administered, the mice were anesthetized, and pupils were dilated with 1% tropicamide for 5 min and kept hydrated with GenTeal. Fluorescence was imaged using a retinal imaging microscope (Micron III, Phoenix Research Labs) using an FF02- 475/50 nm excitation filter (Semrock, Inc.). We observed some variability in optic nerve (ON) fluorescence that could not be readily explained, so the optic nerve was excluded from analyses in all samples.

To determine the natural history of photoreceptor death of *rd10* and *rd10/Serpinf1*$^{-/-}$ mice, we assessed photoreceptor cell death in live mice using the fluorescent probe termed PSVue® 550 to monitor PS externalization by fluorescence fundoscopy (Supplementary Fig. 2). Given the reports about the retinas of *rd10* mice starting to show histological changes at P16, and with a peak in the number of TUNEL+ nuclei in the ONL at P17-18[13], we monitored PS externalization in photoreceptors of these mice undergoing degeneration before death onset. Eye drops of 1 mM PSVue® 550 solution in HBSS were administered to left eyes and HBSS (vehicle) to their contralateral right eyes of each mouse at ages P16, P20, P22 or P24. PS externalization was determined by fluorescence fundoscopy 24 h post-administration. PSVue labeling of phosphatidylserine (PS) externalization associated with photoreceptor cell death in the *rd10* retina (Supplementary Figs. 2, 3).

Retinal cross sections, histology, and immunofluorescence

Both eyes were oriented before enucleation to allow sectioning along the dorsal/ventral axis. Enucleated eyes from *rd10* and *rd10/Serpinf1*$^{-/-}$ mice were incised in the cornea and fixed in 2.5% glutaraldehyde for 20 min and then in 10% neutral buffered formalin at 4 °C for at least 48 h, followed by paraffin embedding, sectioning, and staining with either H&E or immunofluorescence procedures. Slides containing retinal sections were deparaffinized by immersing the slides in various subsequent ethanol dilutions(100%, 95%,70% and 50%), then rinsed with phosphate-buffered saline, pH 7.4 (PBS, Quality Biological, 119-069-101), followed by incubation in blocking buffer containing 0.5% normal donkey serum (Abcam, ab7475), 0.5% bovine serum albumin (BSA, GoldBio, A-420-100), 0.1% Triton X-100 (Sigma, T8787-100) in PBS pH 7.4 for 2 h at room temperature[28]. For fluorescence microscopy, antibodies, and 0.1 µg/ml DAPI were used to immunostain and counterstain the nuclei, respectively. Antibodies used in the study are listed in Supplementary Table 3. Images were acquired using a ZEIS 700 confocal microscope. Fluorescence intensity was quantified using ImageJ, and a rectangle was selected around regions of interest (ROIs), channels were split for multiple antibodies, threshold was adjusted, noise was de-speckled, and fluorescence intensity was measured[28].

Eyes from *Rho*$^{P23H/+}$ mice eyes were enucleated and fixed in Davidson's fix (8% formaldehyde (Merck, cat. F8775), 32% ethanol (Carlo Erba, cat.

414608), 10% acetic acid (Merck, cat. 695092)) over-night. After embedding in paraffin, 14 µm sections were collected. For TUNEL, sections were treated with 0.1 M Citrate Buffer pH 6 (10 mM Tri-sodium citrate (Carlo Erba, cat. 368007)), 0.2 mM citric acid (Merck, cat: 251275) in microwave for 5 min, then labeling was performed for one h at 37 °C using the In Situ Cell Death Detection Kit (Merck, cat. 12156792910). Rod photoreceptors were labeled with anti-RHO 1D4 antibody followed by Alexa Fluor 568 anti-mouse secondary antibody. Cone photoreceptors were labeled with anti-Opsin Blue (Merck, cat. AB5407) and anti-Opsin Red/Green (Merck, cat. AB5405). GFP localization in control transduced retinas was identified with specific anti-GFP antibody and Alexa Fluor 488 anti-mouse secondary antibody. Microglial cell labeling was performed using anti-Iba1 antibody (Wako, cat. 019-19741). For nuclear staining, 0.1 µg/ml DAPI was used. Slides were mounted with Mowiol 4–88 (Merck) and images acquired with a Zeiss Axio Imager A2 fluorescence microscope. To count TUNEL positive cells the RETINA Analysis Tool kit for ImageJ was used[37].

To generate spider plots, the ONL thickness was measured from images passing through the optic nerve (ON) acquired with light microscopy of the retina sections stained with H&E or images of retina sections stained with DAPI with a dorsal-ventral orientation. The ONL thickness in the entire retina sections was measured at 5 different positions from both sides of the ON using ImageJ[28]. Alternatively, for DAPI stained images, a customed macro implemented in ImageJ was used to select only the ONL.

All images from different mice of each genotype and age were collected with identical magnification, gain and exposure settings, and the same retinal region. Each experimental group included at least five eyes.

Retinal functional assessment of *rd10* and *rd10/Serpinf1*$^{-/-}$ mice

Electroretinogram (ERG) for *rd10* and *rd10/Serpinf1*$^{-/-}$ mice were dark-adapted overnight and recorded in both eyes of each animal using an Espion E2 system with ColorDome (Diagnosys LLC) with a heated surface[28]. Briefly, pupils were dilated with 1% tropicamide (Akorn, NDC: 17478-101-12) for 10 min and mice were anesthetized with intraperitoneal injection of Zetamine™ (Ketamine hydrochloride injection, USP; VetOne, NDC 13985-584-10) at 92.5 mg/kg, and AnaSed® (xylazine injection, Akorn Pharmaceuticals, NDC 59399-110-20) at 5.5 mg/kg. Mice were placed on the heated surface and electrodes were placed in the mouth and a subdermal platinum needle electrode was placed in the back of the mouse to serve as ground. Responses were elicited with increasing light impulses with intensity from 0.0001 to 10 cd-seconds per meter squared (cd.s/m^2). Amplitudes for a-wave were measured from stimulus to the trough of the a-wave and b-wave amplitudes were measured from a-wave to b-wave trough or peak. The values from the a and b waves for both eyes were exported to Microsoft Excel to obtained amplitude values for each mouse.

Viral delivery and evaluation of photoreceptor degeneration in the *Rho*$^{P23H/+}$ mouse model

The cDNA encoding H105A was cloned in frame with the signal peptide from Interferon beta[38], to allow secretion of the H105 peptide, in a pAAV2 vector with a CMV promoter resulting in AAV-H105A. The AAV-H105A and AAV-GFP, as control, viruses were generated by InnovaVector (Pozzuoli, NA, Italy)[39]. For AAV2 delivery, *Rho*$^{P23H/+}$ pups at P5 were anesthetized for 2 min in ice. After eyelid opening, 0.5 µl of AAV-H105A (1.9×10^{12} genome copies (GC)/ml) (one eye) or AAV-GFP (in the contralateral eye, 4.5×10^{12} GC/ml) were intravitreally injected with a 34 GA needle Hamilton syringe. A topical cortisone and antibiotic unguent (TobraDex, 0.3% tobramycin + 0.1% dexamethasone, Alcon) was applied immediately after injection and pups were allowed to recover on a warm pad before reintroduction in the cage.

AAV-H105A mRNA expression

Retinas were microdissected and lysed, and total RNA was purified with RNeasy Mini Kit (Qiagen, Hilden, Germany, catalogue number 74104). 200 ng of total RNA were retrotranscribed with iScript cDNA Synthesis Kit (Bio-Rad, Hercules, CA, USA, catalogue number 1725035) following manufacturer's instruction, and cDNA was used for PCR using the following primers: H105A forward (TGCAGAAGTTGGTCGTGAGG), and H105A reverse (GGATTCTGTTCGCTGGATCC). The amplicons were resolved by electrophoresis in a 2% agarose gel stained with 0.5 µg/ml ethidium bromide (Merck), and the 100 bp DNA ladder molecular weight marker (Promega, G2101).

AAV-H105A protein expression

To detect the transduced H105A peptide, we used a custom-made monoclonal recombinant Fab antibody raised against H105A (Bio-Rad AbD Serotec GmbH, Puchheim, Germany). The custom-made antibodies were produced by HuCAL® technology with a FLAG-tag for detection. To assess antibody labelling of H105A, COS-7 cells (ATCC, cat. CRL-1651) were infected with AAV-H105A at 1.9×10^9 GC/ml (Supplementary Fig. 4). Cells were maintained in DMEM 4.5 g/l (Thermo Fisher Scientific, cat. 11960), supplemented with 10% fetal bovine serum (FBS), 100 U/ml penicillin and 100 µg/ml streptomycin (Thermo Fisher Scientific, cat. 15140148) in 5% CO_2 and at 37 °C. At 48 h post-transduction, cells were fixed in 2% paraformaldehyde (PFA) for 10 min and, after blocking with 3% BSA in PBS, were incubated with 10 mg/ml anti-H105A antibody (clone number AbD57564pao) diluted in 1% BSA and 0.1% Tween 20 at 4 °C for 16 h, followed by incubation with secondary antibody, anti-FLAG M2 antibody (Merck, catalogue number F1804) diluted 1:100 in 1% BSA and 0.1% Tween 20 at 25 °C for 2 h and Alexa Fluor 568 anti-mouse as tertiary antibody (Thermo Fisher Scientific, catalogue number A-11004) diluted 1:1000 in 0.1% BSA at 25 °C for 1 h. The specificity of the custom antibody to the H105A peptide was assessed by pre-incubation with 400 µM H105A peptide at 25 °C for 1 h before using it for immunodetection. Localization of synthetic peptide delivered via eye drops and the transduced H105A peptide in retinal cells after AAV-H105A IVT was evaluated by immunofluorescence with the same protocol. Slides were mounted using Mowiol 4-88 (Merck) and images were acquired using an SP8 confocal microscope (Leica, Heidelberg, Germany) with a 63X oil objective, equipped with white-light laser. Viral expression assessments are shown in Supplementary Figs. 4, 5.

Retinal functional assessment in *Rho*$^{P23H/+}$ mice

Electroretinograms for *Rho*$^{P23H/+}$ mice were recorded in both eyes of each animal. Six-month-old mice were dark-adapted overnight and then anesthetized by intraperitoneal injection of 20% urethane in saline solution (0.9% NaCl) at 0.1 ml/10 g of body weight. Pupil were dilated by topical administration of 1% atropine ophthalmic solution[40]. Mice were placed inside a 30 cm diameter Ganzfeld sphere, and coiled gold electrodes were placed in the corneas moistened by a thin layer of gel (Lacrinom, Farmigea, Italy) and the reference electrode (ground) was placed in the scalp. Six calibrated neutral density filters were utilized to regulate the intensity of the light stimulation, which was performed using a white light electric flash (SUNPACK B3600 DX, Tecad Company, Tokyo, Japan). Scotopic ERG responses were registered with increasing light stimuli (0.0041 to 377.2 cd.s/m^2, using 0.6 log units increments) with an inter-stimulus interval spanning from 20 s for dim flashes to 45 s for the brightest flashes. After 15 min from background onset, isolated cone (photopic) components were registered by superimposing the test flashes (0.016 to 377.23 cd.s/m^2) over a stable background of saturating intensity for rods (30 cd/m^2). The amplitude of the scotopic and photopic b-waves was measured from zero to the b-wave peak.

Stem cell-derived retinal organoid generation

We utilized the human-derived induced pluripotent stem cell (hiPSC) cell line A18945 (Gibco), which was sourced from female cord blood. This hiPSC line was cultured on an extracellular Matrigel basement membrane matrix (Corning, 354230) and maintained in mTeSR1 media (StemCell Technologies) until they were 60-70% confluent and ready for differentiation.

Human iPSCs were differentiated into retinal organoids (ROs) following the protocol by Zhong et al.[41]. Briefly, on Day 0, hiPSC colonies were dissociated with dispase and grown in a suspension to form embryoid

bodies, and slowly transitioned to neural induction media (DMEM/F12 (1:1), 1% N2 supplement (Invitrogen), 1 x minimum essential media-nonessential amino acids (NEAAs), 2 µg/ml heparin (Sigma)). On Day 7, EBs were seeded on Matrigel coated plates and maintained in neural induction media. On Day 16, the media was switched to the retinal differentiation medium (DMEM/F12 (3:1), 2% B27 (without vitamin A, Invitrogen), 1x NEAA and 1% antibiotic–antimycotic (Gibco)). Retinal domains were identified and lifted manually with tungsten needles between Day 21 and Day 26 under a phase contrast microscope. On day 30, the culture medium was transitioned to DMEM/F12 (3:1) with 2% B27, 1x NEAA, 1% antibiotic–antimycotic, 10% fetal bovine serum (FBS; Gibco), 100 mM Taurine (Sigma), and 2 mM GlutaMAX (Invitrogen). Additionally, 1 µM retinoic acid supplement was introduced daily starting from day 63. On day 91, the medium was modified to DMEM/F12 (1:1) supplemented with 1% N2, 1 x NEAAs, 1% antibiotic–antimycotic, 10% FBS, 100 mM Taurine and 2 mM GlutaMAX, and the concentration of retinoic acid supplementation was reduced to 0.5 µM for the remainder of the culture period. The use of hiPSCs in this study conforms to the University of Colorado Institutional Biosafety Committee standards.

RO culture treatments

On Day 180, live ROs were individually plated into transparent U-bottom 96-well plates, washed three times with PBS (Gibco, 14190-144) and treated according to each of five experimental conditions: Vehicle Control (DMSO), Cigarette Smoke Extract (CSE) (500 µg/ml) (Murty Pharmaceuticals, NC1560725), CSE with R99A (20 nM), and CSE with H105A (1 nM and 20 nM), for 24 hours at 37 °C in a CO_2 incubator.

Quantitative assessment of cell death in live ROs

After treatment, ROs were washed in PBS (Gibco, 14190-144) and the autofluorescent background was measured by 3D-automated reporter quantification (3D-ARQ)[42], using a Tecan Spark Plate reader (SparkControl v2.3). The Z-position was determined manually by selecting the individual well and fluorescent intensity was measured using the optimized parameters below. ROs were then incubated with 10 µM PSVue-794 (Molecular Target Technologies, P-1001) for 1 h at 37 °C, or with 4 µM of Ethidium Homodimer (Thermo Fischer Scientific, L3224) for 45 min at 37 °C. After incubation, ROs were washed three times with PBS, and fluorescence intensity was measured by 3D-ARQ using the following parameters: Mode: Fluorescent top reading; Wavelength for PSVue-794: Excitation: Emission 730:820 nm, Excitation bandwidth: 10 nm, Emission bandwidth: 15 nm; Wavelength for Ethidium Homodimer: Excitation: Emission 530:630 nm, Excitation bandwidth: 5 nm, Emission bandwidth: 5 nm; Gain: 160, Manual; Number of flashes: 20; integration time: 40 µs; lag time 0 µs. Clear DMEM media was used as a blank. Results were analysed after background subtraction; $n = 19$-24 ROs per condition. Supplementary Fig. 6 shows live retinal organoid staining with cell death indicator dyes.

TUNEL staining

D180 ROs were treated with each of the 5 experimental conditions, as described above ($n = 5$ for each condition), washed with PBS three times, and fixed with 4% paraformaldehyde for 10 min at room temperature. ROs were then subjected to overnight incubation in 6.75%, 12.5% and 25% sucrose solutions in PBS, embedded in Optimal cutting temperature compound (OCT compound, Fisher Healthcare #4585): Sucrose (1:1) solution, and stored at -80 °C. Cryosections of 10 µm were prepared using a Leica Cryostat. Slides were dried and washed with PBS for 15 min. Subsequently, slides were rinsed three times with deionized water for 5 min and incubated in 1X Terminal Transferase (TdT) buffer containing 1X buffer 4 (NEB) and 2.5 µM $CoCl_2$ for 10 min at room temperature in a humid chamber. For labelling, TdT buffer, biotinylated 16 -dUTP and TdT were added to each slide and incubated for 1 h at 37 °C in a humid chamber. The reaction was stopped by incubating slides in 2XSSC (Research Products International Corp. #S24022-1000.0) for 15 min at room temperature followed by a wash with PBS. Blocking was performed using 2% BSA in PBS for 10 min at room temperature, and slides were incubated with streptavidin CY3 (ThermoFisher Scientific #438315) for 45 min at room temperature in a humid chamber. Subsequently, slides were washed 3 times with PBS, counterstained with DAPI for 10 min, washed with PBS and DI water and mounted using FluoroMount solution (SouthernBiotech #0100-01). Fluorescence images were acquired with a Nikon C2 Confocal Microscope A1 (Minato City, Tokyo, Japan) and stitched together using Nikon Elements Software. Images were analysed with Fiji. The relative area of positive immunostaining was calculated as a percentage of total retinal area.

Statistics and reproducibility

We performed each in vivo experiment at least three times and used representative data per treatment and age in the calculations.

Data were analyzed using GraphPad Prism version 10.2.2 for Windows (GraphPad Software). All experimental groups of mice were compared to each other using a paired t-test or One-way ANOVA with Šídák's multiple comparisons test or using Dunette's multiple comparison as we compared the mean of the control group with the other groups. All groups are shown as mean ± SD. p-values lower than 0.05 were considered statistically significant.

Statistical analyses for human ROs were performed using One-way ANOVA using Tukey's multiple comparisons test. p-values less than 0.05 were considered statistically significant. Bar graphs depict the means ± SD with individual values plotted.

Reporting summary

Further information on research design is available in the Nature Portfolio Reporting Summary linked to this article.

Results

Small PEDF peptides delivered via eye drops penetrate into mouse retinas

Previously, we demonstrated that neurotrophic PEDF-derived peptides 17-mer and H105A have affinity for PEDF-R, and that R99A peptide lacks PEDF-R affinity and neurotrophic activity[29]. To evaluate their retinal penetration upon delivery via eye drops, solutions of Alexa Fluor™ 488-conjugated peptides were applied as eye drops to C57BL/6J mice. Peptide penetration into the photoreceptor layer was monitored by fluorescence fundoscopy at time intervals up to 48 h post-administration. After 1-hour, fundi images exhibited high fluorescence intensity, which diminished over time (Fig. 1b). About 10% of applied peptide amounts reached the posterior retina within one hour, with 5% -1% remaining between 6–24 h, respectively, and becoming undetectable by 48 h for all three peptides (Fig. 1c). Peptide distribution in the retina was specific to photoreceptor inner (IS) and outer segments (OS) at 1-hour (Figs. 1d) and 6 h post-administration, increasing the intensities in proportion with their PEDF-R affinity R99A < 17-mer<H105A[29]. While R99A was diffusely distributed, peptides 17-mer and H105A decorated the OS in a punctuated fashion (Fig. 1d) that paralleled the PEDF-R distribution in the retina (Fig. 1e). No visible pathologic changes were noticed in retinas exposed to the PEDF peptides. Because the phospholipase A2 (PLA_2) activity of PEDF-R is critical for the PEDF-mediated photoreceptor protection[27], we determined the PLA_2 activity in response to the PEDF peptides. While the presence of additional PLA_2 enzymes in the mouse retina precluded evaluating the peptides for stimulating PEDF-R in this tissue, assessments using purified recombinant PEDF-R in the presence of peptides showed that only 17-mer and H105A peptides are functional effectors of PEDF-R capable of stimulating its PLA_2 activity (Fig. 1f).

These findings imply that PEDF-R affinity facilitated the localization of peptides at photoreceptors, highlighting the effective bioavailability of 17-mer and H105A peptides delivered as eyedrops to activate PEDF-R in the photoreceptor layer. Additionally, the observed clearance of peptides within 24 hours suggested that daily administration of peptide eye drops might ensure prolonged bioavailability, thereby potentially enhancing their therapeutic efficacy.

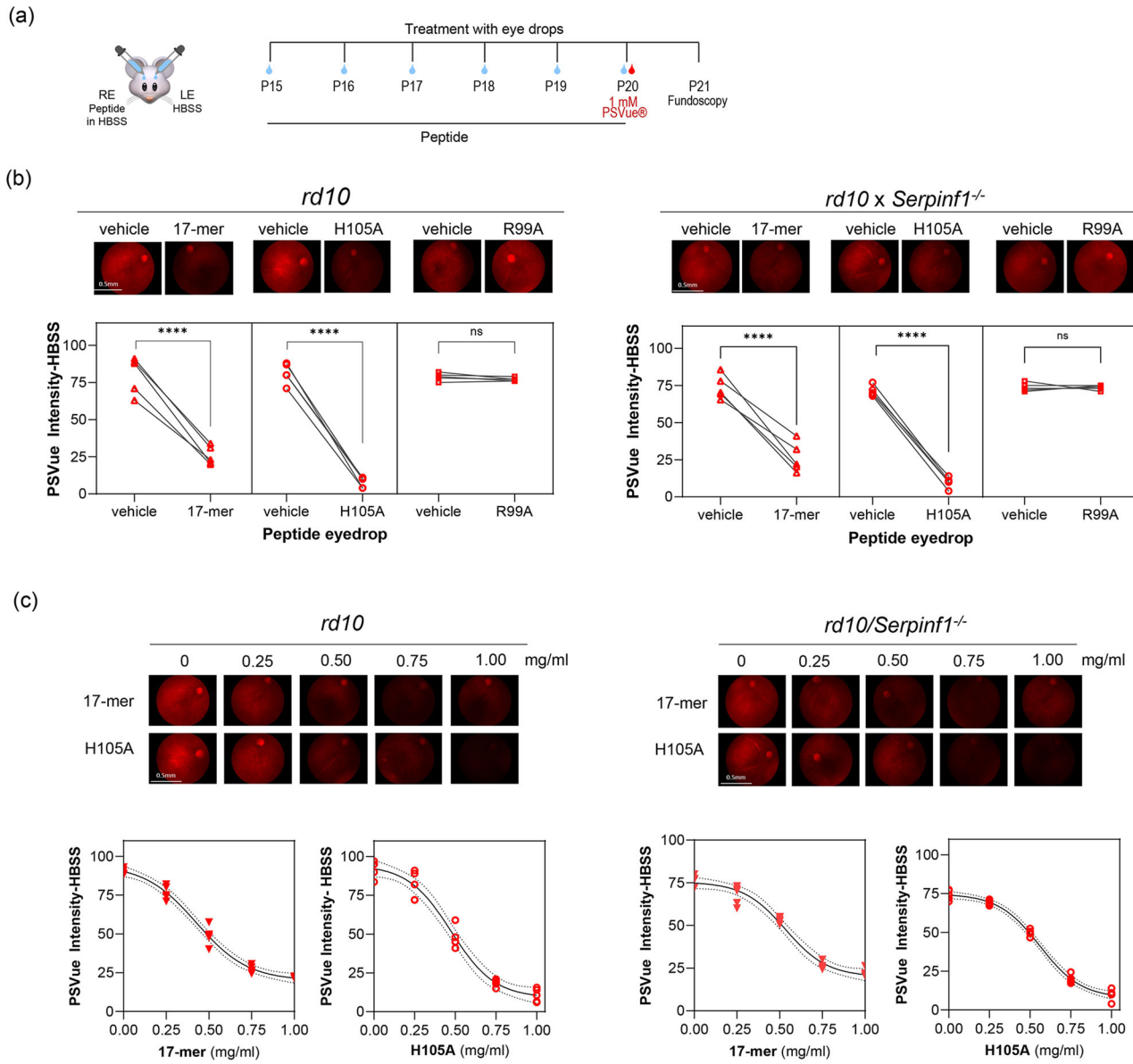

Fig. 2 | Effect of PEDF peptide eye drops on protection against photoreceptor cell death in *rd10* and *rd10/Serpinf1*$^{-/-}$ mice. a Illustration of the experimental timeline of peptide application. Eye drops containing 5 µl of 17-mer, H105A, or R99A peptides in HBSS were administered daily to eyes of *rd10* and *rd10/Serpinf1*$^{-/-}$ mice from P15 to P20. Vehicle (HBSS) was applied in contralateral eyes. At P20, PSVue® was applied via eye drops, and fluorescence fundoscopy was conducted at P21 to assess photoreceptor cell death. RE and LE refer to the right and left eyes, respectively. **b** Fluorescence fundoscopy micrographs. Representative fluorescence fundoscopy images of retinas from mice treated as in Panel **a** with eyedrops of 1 mg/ml of each peptide. Quantification of fluorescence intensity was performed using ImageJ, with average intensity values corrected for background fluorescence from eyes that had not received PSVue or peptides. Each line represents data from one animal comparing treated and contralateral eyes, with five eyes (n = 5) per condition. Statistical significance was determined by paired t-test (****$p \leq 0.0001$, and ns > 0.05). Scale bar = 0.5 mm. **c** Dose response of peptide eye drops. Representative fluorescence fundoscopy micrographs showing retinas treated with varying concentrations of 17-mer and H105A peptides (0.0 mg/ml to 1.0 mg/ml) in *rd10* and *rd10/Serpinf1*$^{-/-}$ mice. Fluorescence intensity was quantified and analyzed using Sigmoidal interpolation in GraphPad. Each data point represents the average of three images per retina, with a total of five retinas (n = 5) per condition.

Eye drops of 17-mer and H105A peptides prevent photoreceptor death in *rd10* mouse models of RP

Phosphatidyl serine (PS) externalization by phospholipid translocases provides an emblematic eat-me signal in apoptotic cells for efferocytosis. This has been exploited for detecting rat photoreceptor cell death in vivo using the PSVue®-550 fluorescent probe, which contains a bis(zinc2^{+}dipicolylamine) (Zn-DPA) group that selectively binds to cell membranes enriched with exposed PS phospholipids in apoptotic and necrotic cells[36,43]. We optimized this method to monitor PS externalization in photoreceptors of *rd10* and *rd10/Serpinf1*$^{-/-}$ mice starting at P16, when their retinas start showing histological changes consistent with retinal degeneration[13], until P25 in vivo, when most of the photoreceptors have died (Supplementary Fig. 2). We found that PS externalization agreed with the natural history of photoreceptor death, and selected P21 as the endpoint for PS externalization monitoring in vivo.

To evaluate the efficacy of eye drops containing 17-mer, H105A and R99A peptides in delaying PS externalization in both *rd10* and *rd10/Serpinf1*$^{-/-}$ mouse models in vivo, animals received daily eye drops starting at P15 before photoreceptor death onset. Treatment continued until P20, when PSVue®-550 was also applied, and fundoscopy was performed at P21 (Fig. 2a). The results demonstrated that eye drops containing 17-mer or H105A diminished fundi fluorescence, indicating lower PS externalization compared to the vehicle (HBSS) eye drops. Notably H105A peptide was more effective than 17-mer, while R99A peptide showed no major efficacy

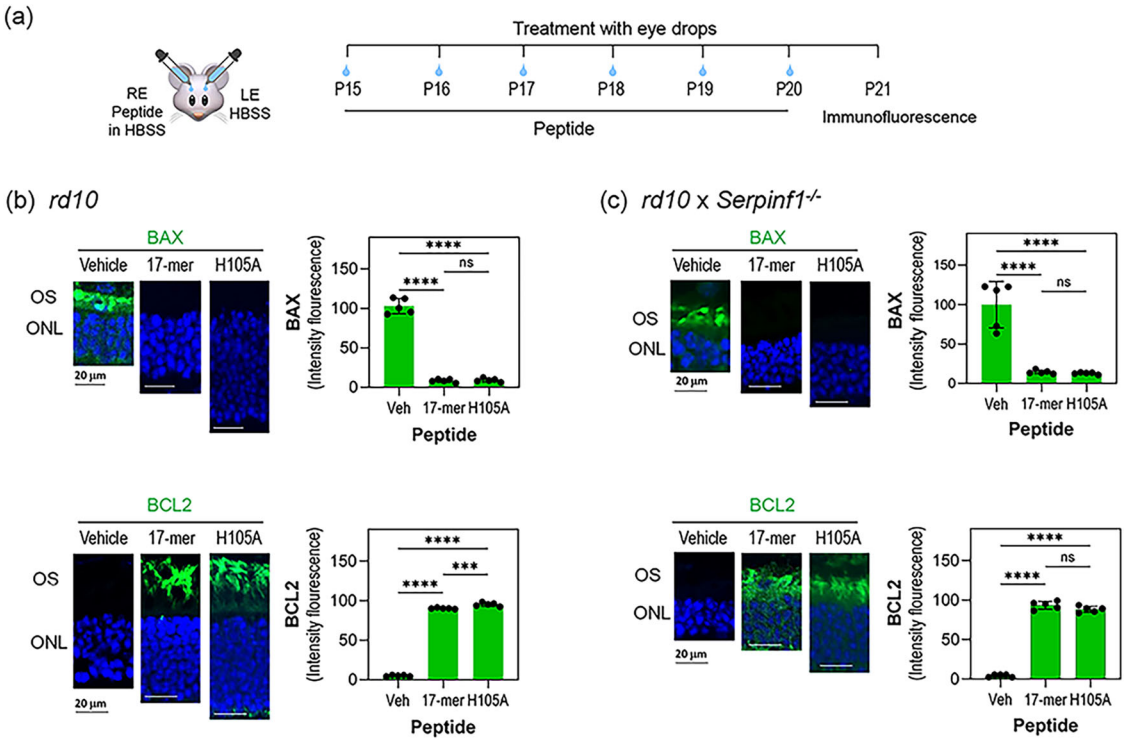

Fig. 3 | Eyedrops of 17-mer and H105A peptides decrease the BAX/BCL2 ratio in photoreceptors of *rd10* and *rd10/Serpinf1*$^{-/-}$ mice. a Illustration of the experimental timeline of peptide application. RE and LE refer to the right and left eyes, respectively. Immunostaining of retinas. Representative fluorescent micrographs of retinas from *rd10* (**b**) and *rd10/Serpinf1*$^{-/-}$ (**c**) mice treated with 17-mer or H105A peptides at 1 mg/ml via eye drops, along with vehicle-treated controls. Immunostaining was performed with antibodies against BAX or BCL2 (green), and DAPI (blue). Histograms show quantification of immunofluorescence intensity for BAX and BCL2 markers. Five retinas ($n = 5$) per group were analyzed, with two sections per retina. Each individual data point represents the average of intensity from two sections per retina, with statistical significance determined by ANOVA Šídák's multiple comparisons test. ***$p \le 0.001$, ****$p \le 0.0001$, ns $p > 0.05$. Presented as average of the five retinas ± SD. Scale bar = 40 µm.

(Fig. 2b). Further titration experiments with 17-mer and H105A peptides revealed concentrations as low as 0.5 mg/ml were effective in restraining PS externalization in photoreceptors in both RP mouse models (Fig. 2c). This demonstrates the benefit of both 17-mer or H105A peptide eye drops in blocking PS externalization, an early step in the cell death process. For subsequent experiments, a working dose of 1 mg/ml peptide was used.

Given that intravitreal injections of PEDF protein, 17-mer or H105A peptides elevate anti-apoptotic BCL-2 and attenuate pro-apoptotic BAX levels in photoreceptors of retinal degeneration models such as the *rd1* mouse and RCS rat[30,44], we hypothesized that these peptides delivered via eye drops would similarly regulate BCL-2 and BAX proteins to prevent cell death in *rd10* and *rd10/Serpinf1*$^{-/-}$ retinas. To test this hypothesis, we assessed the distribution of BAX and BCL2 proteins in photoreceptors of *rd10* and *rd10/Serpinf1*$^{-/-}$ mice following the application of peptide eye drops. Our results showed that both 17-mer and H105A eye drops decreased BAX and increased BCL2 levels in the photoreceptors in both RP models (Fig. 3a–c, Supplementary Figs. 2d).

Together, the findings indicate that daily treatments with 17-mer or H105A peptide eye drops effectively protected *rd10* and *rd10/Serpinf1*$^{-/-}$ mice against photoreceptor cell death, demonstrating the potential of these peptides as a non-invasive approach for RP.

Eye drops of 17-mer and H105A peptides improve photoreceptor morphology and function in *rd10* mouse models

Early changes effected by RP can be histologically detected as shortening of photoreceptor OS and photoreceptor loss. Histological examination showed that retinas of *rd10* and *rd10/Serpinf1*$^{-/-}$ mice treated with daily H105A or 17-mer peptide eye drops had longer OS and thicker outer nuclear layer (ONL, containing photoreceptor cells) than vehicle-treated or untreated eyes, while R99A had no effect at P21 (Fig. 4a–c). In *rd10* mice, H105A or 17-mer peptide eye drops restored ONL thickness, with H105A to almost wild-type levels (Fig. 4b, d; spider plots). In *rd10/Serpinf1*$^{-/-}$, ONL preservation was less marked (Fig. 4c, e), likely due to the increased retinal degeneration susceptibility caused by *Serpinf1* gene deletion[16]. Again, vehicle- and R99A-treated eyes were inefficient in restoring ONL thickness.

RP is associated with reduced or delayed electrical responses to light. Electroretinography (ERG), the standard technique for assessing retinal dysfunction associated with RP and for measuring RP treatment outcomes, was performed to evaluate the functional effects of 17-mer or H105A eye drops in *rd10* and *rd10/Serpinf1*$^{-/-}$ mice. ERG a-wave and b-wave responses are indicative of photoreceptor function, and of post-synaptic activation of bipolar cells by photoreceptors, respectively. In dark-adapted *rd10* and *rd10/Serpinf1*$^{-/-}$ mice at P21, the peptides elicited a- and b-wave responses that increased exponentially with light stimuli between log(-0.01) and log(10) cd.s/m^2, indicating that, relative to vehicle-treated eyes, the PEDF-derived peptides protected visual function (Fig. 5). Application of H105A peptide eye drops every other day and extending the endpoint to P25, when most photoreceptors degenerate, also improved the function of *rd10* photoreceptors, with modestly lower efficacy than daily treatments and a shorter endpoint (Supplementary Fig. 7).

These findings show the ability of H105A or 17-mer peptide eye drops to limit photoreceptor cell morphology changes and loss, to improve electrical light responses in both mouse models, and thus delay retinal degeneration.

H105A peptide eye drops promote photoreceptor survival and improve morphology of the ONL in the *Rho*$^{P23H/+}$ mouse model of RP

We evaluated the efficacy of eye drops containing the H105A peptide in preventing photoreceptor cell death in the *Rho*$^{P23H/+}$ mouse model of

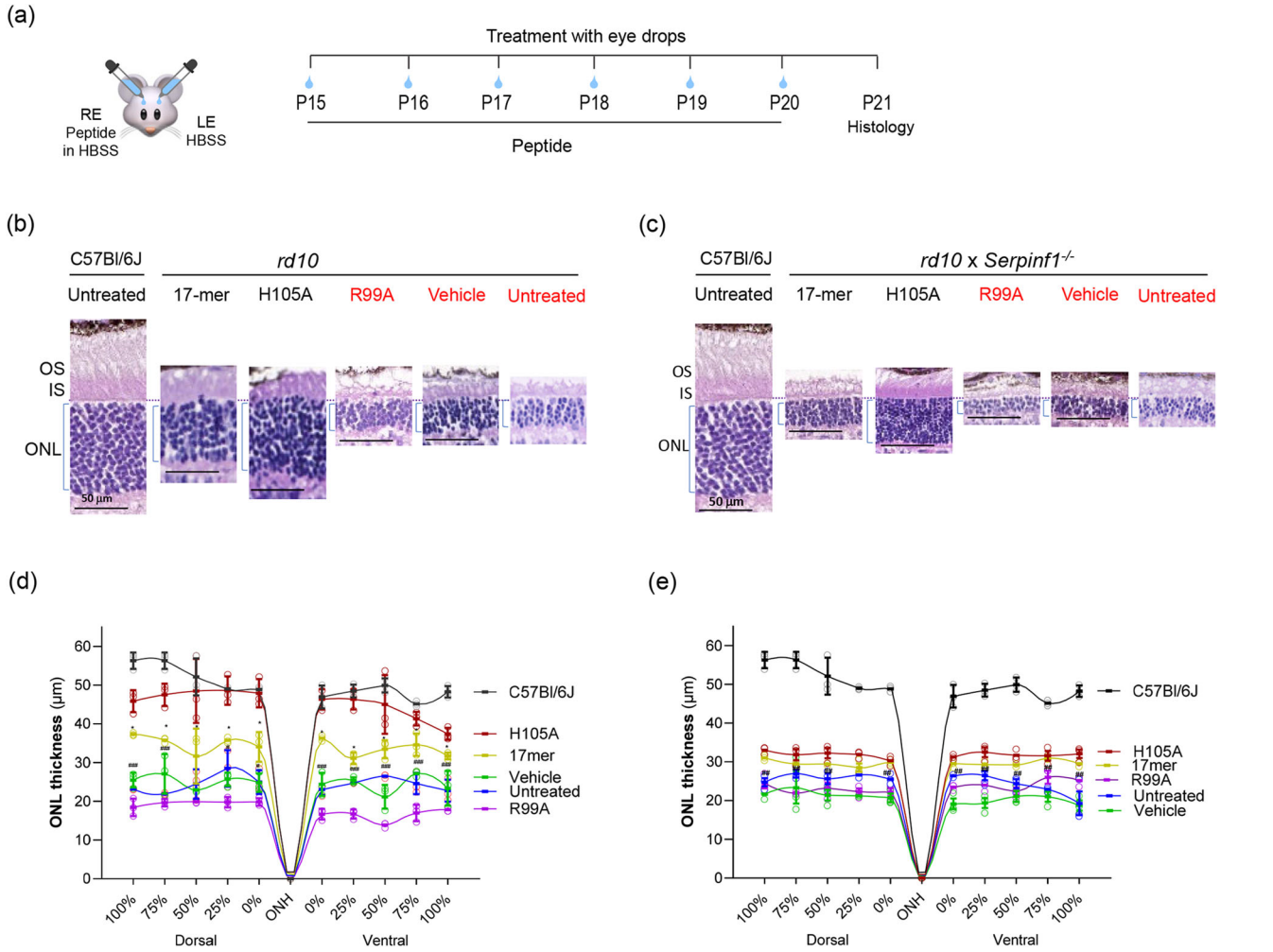

Fig. 4 | Effect of eyedrops of 17-mer and H105A peptides on photoreceptor morphology of *rd10* and *rd10/Serpinf1*$^{-/-}$ mice. a Illustration of the experimental timeline of peptide application. RE and LE refer to the right and left eyes, respectively. Histological Evaluation. Representative microphotographs of retina sections from *rd10* (**b**) and *rd10/Serpinf1*$^{-/-}$ (**c**) mice treated with 17-mer, H105A, or R99A peptides at 1 mg/ml, or with vehicle (HBSS), compared to wild type C57BL/6 J mice. Sections were stained with hematoxylin and eosin. Spider Plot illustrate the thickness of the outer nuclear layer (ONL) in *rd10* (**d**) and *rd10/Serpinf1*$^{-/-}$ (**e**) mice. Five retinas ($n = 5$) per group were analyzed and each data point represents the average ± SD per location relative to the optic nerve (ON), analyzed using One-way ANOVA with Šídák's multiple comparisons test. Statistics for comparisons between H105A and vehicle is indicated by #$p \le 0.05$, ##$p \le 0.01$, and ###$p \le 0.001$, and between H105A and 17-mer by *$p \le 0.05$. Scale bar = 50 µm.

RP, which exhibits a slower progression of photoreceptor degeneration compared to *rd10* mice. Starting from P14—prior to the onset of photoreceptor death in *Rho*$^{P23H/+}$ mice[45]—H105A peptide eye drops were administered daily through P19, with contralateral control eyes receiving vehicle HBSS (Fig. 6a). This treatment resulted in penetration of the eye-drop-delivered H105A to the retina, reaching the photoreceptors (Supplementary Fig. 5c), and led to attenuation of BAX levels and increases in BCL2 at P19, suggesting inhibition of apoptotic pathways and activation of survival mechanisms mediated by the H105A peptide (Fig. 6b). At P19, preservation of ONL thickness was already visible in the ventral retina, a region where degeneration typically progresses more rapidly in this RP model[17] (Fig. 6c). Quantification of ONL thickness via spider graph confirmed this preservation in the ventral retina (Fig. 6d). Additionally, the outer segments (OS) of rod photoreceptors, labeled by rhodopsin, were preserved with H105A treatment (Fig. 6e).

Overall, these findings demonstrate that H105A peptide eye drops effectively promote photoreceptor survival and preserve retinal structure in the *Rho*$^{P23H/+}$ mouse model of RP, particularly in retinal regions more vulnerable to degeneration, such as the ventral retina. This supports the potential of H105A as a therapeutic approach for retinal degenerative diseases caused by various genetic mutations.

Delivery of H105A by AAV transduction protects photoreceptors in the *Rho*$^{P23H/+}$ mouse model of RP

To assess the longer-term effects of H105A peptide, we developed a gene therapy-based delivery system for sustained expression of H105A. We selected the adeno-associated virus serotype 2 (AAV2) due to its efficacy in transducing retinal cells, making it well-suited for treating ocular disorders[46]. AAV2 is a well-established and FDA-approved viral vector. Since the therapeutic agent is secreted extracellularly and does not require direct expression by photoreceptors, we opted for intravitreal (IVT) injection. This method is safer than subretinal delivery as it avoids the risk of retinal detachment. Additionally, IVT injection targets cells across the entire retina providing a broader area of treatment compared to the localized effect of subretinal injections.

A single IVT of AAV-H105A was administered to the eyes of mice at P5, with a control AAV-GFP IVT injection in the contralateral eye (Fig. 7a). By P19 and P180, cells transduced with AAV-H105A expressed viral mRNA and produced the neuroprotective agent in the retina

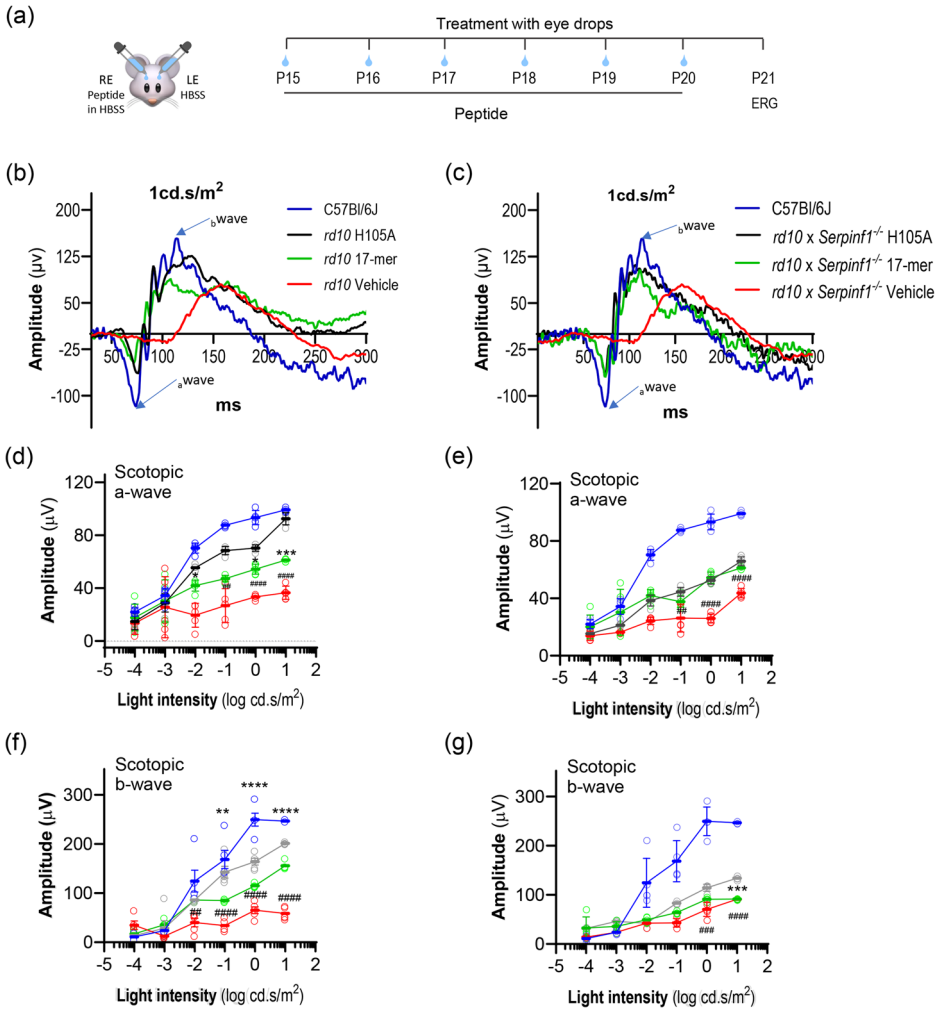

Fig. 5 | Effect of daily eyedrops of PEDF peptides on ERG a-wave and b-wave retinal function. **a** Illustration of the experimental timeline of peptide application. RE and LE refer to the right and left eyes, respectively. Representative ERG waveforms for *rd10* (**b**) and *rd10/Serpinf1*$^{-/-}$ (**c**) mice at P21 in response to a light flash (1 cd.s/m²). Amplitude (y-axis) is plotted against time in milliseconds (ms, x-axis). Treatments are indicated to the right of each plot and are color coded, with control wild type C57BL/6 J mice without peptide treatment shown in blue. A-wave and b-wave are indicated by arrows. Photoreceptor a-wave amplitudes. Averages of photoreceptor a-wave amplitudes for *rd10* (**d**) and *rd10/Serpinf1*$^{-/-}$ (**e**) mice as a function of light intensity (cd/s.m², x-axis). Responses of animals treated with 17-mer are shown in green, H105A in black, and vehicle (HBSS) in red. Wildtype responses are shown in blue. Bipolar cell b-wave amplitudes. Averages of bipolar cell b-wave amplitudes for *rd10* (**f**) and *rd10/Serpinf1*$^{-/-}$ (**g**) mice as a function of light intensity (cd/s.m², x-axis), with treatments as indicated in panels. The number of mice evaluated for the data shown in Panels **d**-**g** was five ($n = 5$) for each *rd10*, *rd10/Serpinf1*$^{-/-}$ and wild type. Each data point represents the average ± SD of each genotype, analyzed by ANOVA with Dunnett's multiple comparisons. Statistical significance between H105A and vehicle is indicated by ##$p \le 0.01$, ###$p \le 0.001$, ####$p \le 0.0001$, and between H105A and 17-mer by **$p \le 0.01$, ***$p \le 0.001$, ****$p \le 0.0001$.

(Supplementary Figs. 4, 5). At P19, AAV-H105A reduced inflammation, as detected by decreased Iba1+ cells in the photoreceptor layer (Fig. 7b). The treatment decreased BAX levels and increased the BCL2 levels (Fig. 7c). Additionally, it reduced the percentage of TUNEL-positive photoreceptor nuclei compared to GFP controls (Fig. 7d), indicating that AAV-H105A IVT protected the *Rho*$^{P23H/+}$ retinas against photoreceptor cell loss. Retinal assessments at P19 and P180 revealed slightly thicker ONL and better preservation of rhodopsin and cone opsins staining in the OS, which label rods and cones, respectively, in eyes producing H105A compared to GFP (Fig. 7e, f). Functional evaluations using ERG demonstrated improved b-wave responses in both scotopic (rods) and photopic (cones) conditions, with improvement in rod function and slight improvement in cone function six months after AAV delivery (Fig. 7g, h).

These results underscore the multifaceted benefits of H105A peptide delivery, including enhanced photoreceptor survival, improved morphology, and augmented light responses in the *Rho*$^{P23H/+}$ model of RP, especially considering the model's slow progression of photoreceptor degeneration.

PEDF-derived H105A peptide promotes retinal cell survival in hiPSC-derived human retinal organoids

To further demonstrate the efficacy of the H105A peptide in promoting retinal photoreceptor and neuronal survival, we used human induced pluripotent stem cell (hiPSC)-derived retinal organoid (RO) technology. RO models mimic the native retinal three-dimensional structure and cellular makeup, including photoreceptors with inner and outer segments, and light responsiveness[41]. To generate a disease-relevant paradigm of photoreceptor cell death, we cultured human ROs up to 180 days of differentiation (D180), a time at which the ONL is well developed, and all photoreceptor subtypes have been specified and are relatively mature[41,47] and treated them with cigarette smoke extract (CSE), a potent oxidant commonly used to induce macular degeneration-related damage in retinal cultures[47–50]. Although RP is a hereditary disease, non-genetic factors, such as oxidative stress, play a central role in its pathogenesis and progression[18–21]. ROs were simultaneously treated with CSE and with H105A or the R99A control peptide (Fig. 8a, b), using CSE alone or vehicle (DMSO) as controls.

Using 3D-ARQ, a technique we previously developed to quantify fluorescence intensity in live 3D ROs[42], we evaluated PSVue®-794 staining in peptide-treated ROs and found that H105A treatments decreased PS externalization in CSE-exposed ROs, relative to CSE alone and CSE + R99A treatments (Fig. 8c). Moreover, H105A prevented CSE-induced cell-death in human ROs as shown using ethidium homodimer, a membrane-impermeable fluorescent dye that binds to DNA in dead or dying cells. H105A treatment decreased CSE-induced cell death relative to treatments with CSE alone and CSE + R99A (Fig. 8d). Consistently, to detect DNA fragmentation occurring in late apoptosis, TUNEL assays were performed in cryosections of D180 ROs treated as described above. H105A treatments decreased the number of TUNEL-positive nuclei in the ONL of ROs undergoing CSE-induced cell death to levels as observed for the untreated ROs (Veh) (Fig. 8e, f).

Altogether, our findings demonstrated that the H105A peptide promoted the survival of human retinal photoreceptors in ROs, highlighting again its translational potential for medical and therapeutic applications related to retinal diseases.

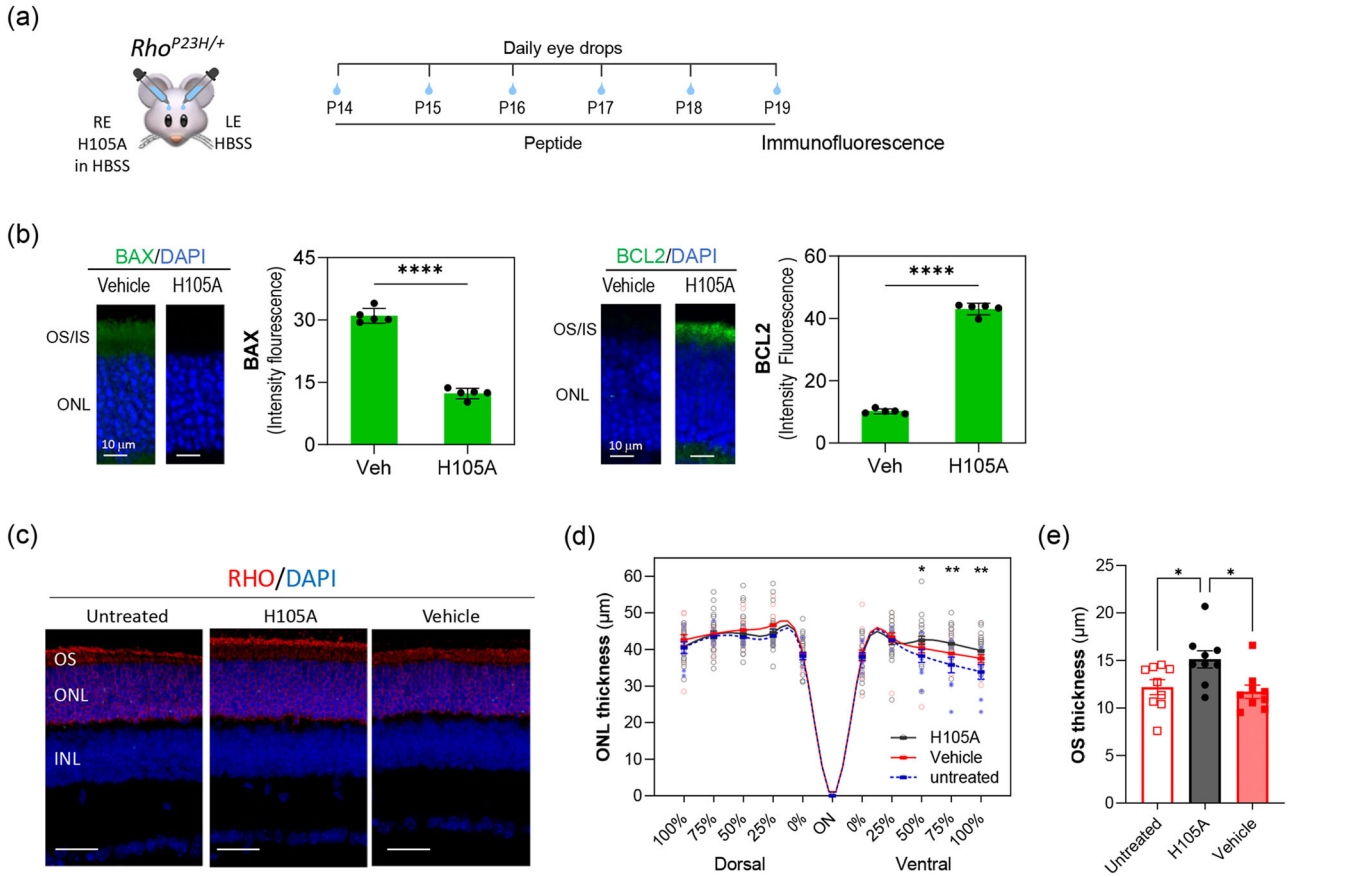

Fig. 6 | Effects of eye drops containing H105A peptide in the photoreceptors of *Rho*$^{P23H/+}$ mice. a Scheme of experimental design. Daily peptide eye drops (5 µl of 1 mg/ml peptide) were applied to mice starting at P14 until P19 when immunofluorescence of retinal cross sections was performed. The contralateral control eyes were treated with vehicle HBSS. RE and LE refer to the right and left eyes, respectively. **b** Immunostaining was performed with antibodies against BAX or BCL2 (green), and DAPI (blue). Histograms show quantification of immunofluorescence intensity for BAX and BCL2 markers. Five retinas per group were analyzed, with two sections per retina. Each individual data point represents the average of five ($n = 5$) retinas ± SD, with statistical significance determined between H105A and vehicle by paired *t*-test (****$p < 0.0001$). Scale bar = 10 µm. **c** Assessment of ONL and OS at P19, labelled by rhodopsin (red), revealed preservation upon H105 peptide exposure. **d** Quantification of ONL thickness represented in the spider plot confirms preservation in the ventral retina. Each data point corresponds to the average ± SD, with statistical analysis performed using One-way ANOVA with Šídák's multiple comparisons for each group presented as average ± SEM. Statistical significance between H105A and untreated is indicated by *$p \leq 0.05$, and **$p \leq 0.01$. The numbers of retinas per condition were: twenty-four ($n = 24$) for H105A, fifteen ($n = 15$) for HBSS, and nine ($n = 9$) untreated retinas. **e** Quantification of OS thickness labelled by rhodopsin shows preservation of photoreceptor OS with H105A peptide treatments. $n = 9$ for each condition. Presented as average ± SD, with statistics performed using One-way ANOVA Šídák's multiple comparisons test. *$p \leq 0.05$

Discussion

Building upon our previous findings on structure-activity relationships of PEDF, in this study we investigated the potential use of small peptides derived from the neurotrophic active region of PEDF delivered as eye drops as a treatment option for RP. We report that 17-mer and H105A peptides, each composed of 17 amino acid residues, act as neurotrophic agents that preserve photoreceptor viability, morphology, and function in models of retinal degeneration mimicking human RP. Our study demonstrates that these peptides, when locally delivered to the eye, achieve sufficient retinal bioavailability to effectively target PEDF-R, the PEDF receptor crucial for photoreceptor survival[27,28]. Consequently, they interfere cell death pathways associated with retinal diseases. Key findings supporting these conclusions include: 1) the 17-mer and H105A peptides target murine photoreceptors and activate PEDF-R when delivered via eye drops or intravitreal AAV2-viral injections; 2) these peptides block PS externalization and DNA fragmentation and increase the BCL2/BAX ratio in photoreceptors of mutant mice undergoing spontaneous cell death; and 3) the peptides improve both the morphology and function of degenerating murine photoreceptors. Peptides showing poor penetration (e.g., 29-mer, Supplementary Fig. 8) and those lacking PEDF-R affinity (e.g., R99A) were ineffective. Additionally, the results obtained using a human retinal organoid model undergoing oxidative stress-induced cell death provide proof-of-concept for the efficacy of the H105A peptide in preventing damage to human retinal cells, further supporting its translational potential for retinal degenerative diseases. Altogether, the findings strongly emphasize the potential of peptide therapeutic approaches for preserving or enhancing vision in retinal degenerative diseases.

The significance and potential impact of our study are grounded on its translational promise as it demonstrates the ability of 17-mer and H105A peptides to stabilize the progression of photoreceptor degeneration in preclinical murine models of human retinal diseases. These peptides show potential to overcome the challenging genetic heterogeneity characterizing RP as demonstrated in distinctive models: the *rd10* containing an alteration in the visual transduction enzyme PDE6, and the *Rho*$^{P23H/+}$ characterized by an alteration in the light receptor rhodopsin protein, modelling different types of human RP; and the *rd10/Serpinf1*$^{-/-}$, a more aggressive variant of the *rd10* model lacking PEDF; as well as human hiPSCs-derived retinal organoids undergoing oxidative stress, a feature of RP[12,16,18]. Not only did the peptides act on preserving photoreceptor morphology but also on improving the light responses of both types of photoreceptors, rods, and

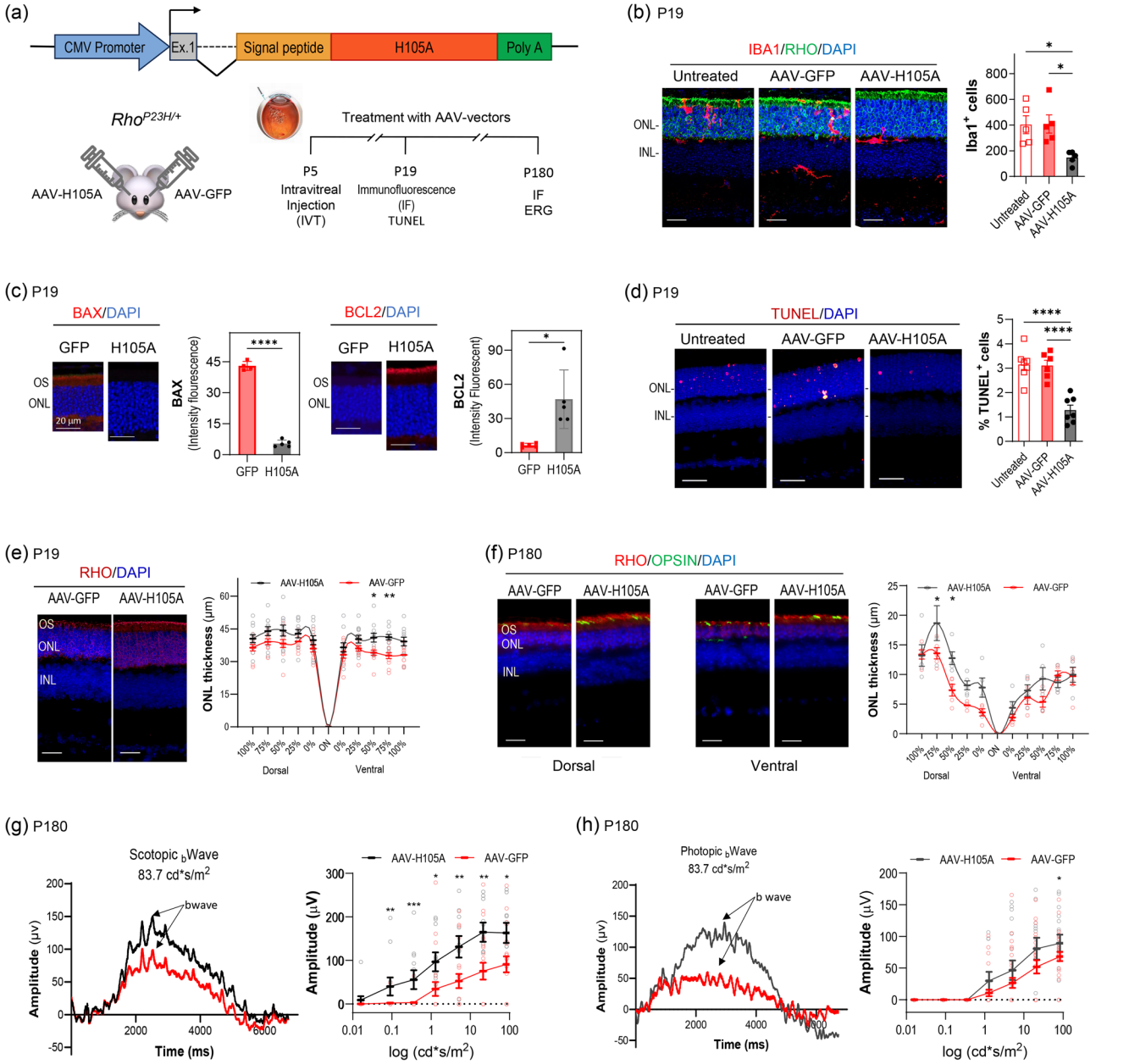

Fig. 7 | Effect of AAV-H105A intravitreal injection on the *Rho*$^{P23H/+}$ mouse model of RP. a Scheme for the experimental design illustrating the cDNA construct containing the secretion signal peptide of interferon beta in frame with the H105A coding sequence under the control of the CMV promoter in the AAV vector. One single IVT injection of 0.5 µl of AAV-H105A (1.9×10^{12} GC/ml) or AAV-GFP (4.5×10^{12} GC/ml) (as control) was administered in eyes of *Rho*$^{P23H/+}$ mice at P5. Assessments were performed at P19 and P180 by immunofluorescence, and TUNEL of retina sections, and at P180 by ERG in live animals. **b** Immunostaining of retinal cross-sections of *Rho*$^{P23H/+}$ mice at P19 and P180 treated with AAV-vectors as described in Panel **a**, showing Iba1^{+} microglia cells (red), rhodopsin (green), with nuclei stained with DAPI (blue). Quantification of Iba1^{+} microglia cells in the retinal layers is shown on the right-hand side. Five retinas per group were analyzed and data are represented as average ± SD, with statistical analysis performed using One-way ANOVA with Dunnett's multiple comparisons test for each group.: $^{**}p \le 0.01$; $^{****}p \le 0.0001$. Scale bar: 20 µm. **c** Immunostaining of retinal cross-sections of mice at P19, treated as described in Panel **a**, with antibodies to BAX or BCL2 (red), as indicated, and with DAPI (blue). Histograms show quantification of the fluorescence signal. Five retinas per group were analyzed, with two sections per retina. Each data point corresponds to the average ± SD, with statistical analysis performed using Paired *t*-test for each group.: $^{**}p \le 0.01$; $^{****}p \le 0.0001$. Scale bar: 20 µm. **d** TUNEL of retinal cross-sections of mice at P19 treated as described in Panel **a**, showing TUNEL-positive cells (red) with DAPI (blue). Histograms show quantification of the percentage of TUNEL+ photoreceptors. The number of retinas per group analyzed per condition were seven (7) untreated, seven (7) AAV-H105A treated, and six (6) AAV-GFP treated. Each data point corresponds to the average ± SD, with statistical analysis performed using ANOVA with Dunnett's multiple comparisons test for each group.: $^{*}p \le 0.5$, $^{****}p \le 0.0001$. Scale Bar: 20 µm. **e** and **f** ONL thickness in retinas treated as described in Panel **a**, assessed at P19 (**e**) and P180 (**f**), on retinal cross-sections stained with DAPI (blue) and anti-rhodopsin (red). Spider plots for ONL thickness as a function of distance from the optic nerve (ON) are shown. Average ± SEM (panel e) and average ± SD (panel f). For ONL thickness, One-way ANOVA with Šídák's multiple comparisons for each group was used $^{*}p \le 0.05$. Scale Bar: 20 µm. Visual function assessment by ERG recording at P180 under scotopic (**g**) and photopic (**h**) conditions. Sensitivity curves in terms of b-wave amplitude in response to different light stimuli are shown. Each data point corresponds to the average ± SEM, with statistical analysis performed using One-way ANOVA with Dunnett's multiple comparisons test for each group. For Panel **g**, $n = 21$ for AAV-GFP; $n = 11$ for AAV-H105A; Luminance (log cd*s/m2) 0,09 $^{**}p = 0.01393$; Luminance (log cd*s/m2) 0.360, $^{**}p = 0.00261$; Luminance (log cd*s/m2) 1.290, $^{*}p = 0.02936$; Luminance (log cd*s/m2) 5.120, $^{**}p = 0.01037$; Luminance (log cd*s/m2) 21.20, $^{**}p = 0.00787$; Luminance (log cd*s/m2) 83.70, $^{*}p = 0.02455$. For Panel **h**, $n = 30$ for AAV-GFP; $n = 17$ for AAV-H105A; Luminance (log cd*s/m2) 83.70, $^{*}p = 0.0408$.

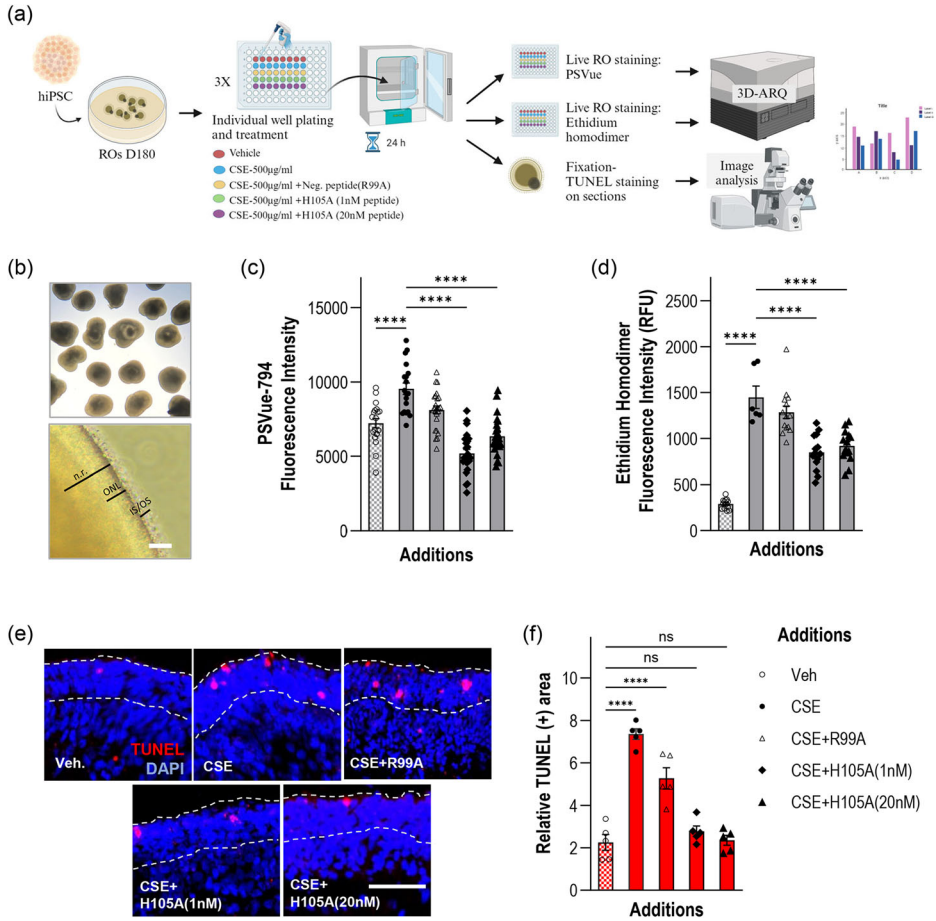

Fig. 8 | Effect of H105A peptide on CSE-induced retinal cell death in human iPSC-derived retinal organoids. a Diagram of Experimental Design. Human ROs at 180 days of differentiation (D180) were treated with vehicle (DMSO), CSE(500 µg/ml), CSE + R99A(20 nM), CSE + H105A(1 nM), or CSE + H105A(20 nM) for 24 h, and cell death was assessed by PSVue794 or Ethidium homodimer staining of live organoids or by TUNEL staining in fixed RO sections. Diagram created with BioRender.com. **b** Representative image of retinal organoids. Top panel shows a representative bright field image of ROs at D180. Bottom panel is a close-up of a D180 RO showing neural retina (n.r.), outer nuclear layer (ONL), and inner and outer segment structures of photoreceptors (IS/OS). Scale Bar: 50 µm. **c** PSVue794 fluorescence intensity (RFU) of PSVue794 in live ROs under the 5 experimental conditions. CSE increases early apoptotic events, evidenced by a statistically significant increase in PSVue794 intensity compared with Vehicle control, and H105A prevents this increase at both tested concentrations. CSE + H105A(1 nM) = 5185.2 ± 275.4 (n = 24) and CSE + H105A(20 nM) = 6342.7 ± 261.3 (n = 24), vs. CSE alone = 10172.6 ± 431.0 (n−19) and CSE + R99A(20 nM) = 8112.5 ± 266.2 (n = 24); Vehicle (n = 19). Mean ± SD; ****p < 0.0001, One-way ANOVA with Tukey's multiple comparisons test for each group. **d** Fluorescence intensity (RFU) of Ethidium homodimer in live ROs under each treatment condition. CSE increases cell death, evidenced by a statistically significant increase in fluorescence intensity compared with Vehicle control, and H105A decreases CSE-induced cell death at both tested concentrations. CSE + H105A(1 nM) = 848.9 ± 51.0 (n = 14) and CSE + H105A(20 nM) = 919.2 ± 46.0 (n = 14), vs. CSE alone = 1447.7 ± 175.3 (n = 6) and CSE + R99A(20 nM) = 1283.2 ± 67.6 (n = 14); Vehicle (n = 13). Mean ± SD; ****p < 0.0001, One-way ANOVA Tukey's multiple comparisons test for each group. **e** Representative photomicrographs of retinal organoid sections stained with TUNEL to assess apoptosis-induced DNA fragmentation. Dashed lines demarcate ONL. Scale Bar: 50 µm. **f** Histogram of quantification of TUNEL staining shows a statistically significant increase in cell death in CSE-treated ROs compared to vehicle controls, and a statistically significant decrease in CSE-induced cell death by H105A treatments. Relative TUNEL(+) area: CSE + H105A(1 nM) = 2.77 ± 0.25 (n = 5) and CSE + H105A(20 nM) = 2.35 ± 0.23 (n = 5), vs. CSE alone=7.36 ± 0.25 (n = 5) and CSE + R99A(20 nM) = 5.27 ± 0.50 (n = 5); Vehicle (n = 5). Mean ± SD; ****p < 0.0001, ns = 0.8045 for Veh vs. CSE + H105A(1 nM); ns = 0.9996 for Veh vs. CSE + H105A(20 nM), One-way ANOVA with Tukey's multiple comparisons test for each group.

cones. These genetically distinct models have common and unique retinopathies, suggesting that the H105A peptide appears to have broad applicability for a range of human retinal diseases involving photoreceptor degeneration. This is primarily due to its ability to target intracellular calcium, a common feature in photoreceptor degeneration[18]. We envision that the H105A peptide would be a beneficial therapeutic agent for other diseases that result in photoreceptor degeneration, including but not limited to other RP types, age-related macular degeneration, choroideremia, Usher syndrome, Stargardt disease, diabetic retinopathy, etc. Further assessments of H105A peptides will be required to identify potential benefits for these and other diseases characterized by photoreceptor degeneration.

To the best of our knowledge, the novelty of this study is highlighted by the use of the neurotrophic H105A peptide therapeutic delivered through eye drops, which offers a high safety profile and multiple delivery options. Peptide eye drops are a compelling alternative to gene-therapy approaches requiring intraocular injections. Eye drop administration is simpler, less invasive, and poses lower risk of retinal damage, which could improve patient compliance. Although several attempts to develop eye drop delivery for retinal disorders have been unsuccessful due to membrane barriers and drug digestion at the eye surface[5], there are promising precedents. For example, a small cyclic peptide of 5 residues, Vasotide, delivered via eye drops effectively reached the posterior ocular tissues to inhibit retinal and choroidal angiogenesis in mice and monkeys[51]. Additionally, in a pilot study, topical administration of nerve growth factor eye-drops in RP patients was found to be safe with some patients experiencing improvements in visual performance[52]. Our findings show successful delivery of therapeutic

peptides via eye drops, with both 17-mer and H105A peptides reaching the posterior retina, the primary site of photoreceptor degeneration in RP. We propose that eye drop delivery could be further enhanced with carrier systems such as nanoparticles, or liposomes, which could improve the stability and bioavailability of PEDF neurotrophic peptides. Moreover, peptide eye drops could serve as an early intervention while gene-targeted therapies are developed for individual patients.

As far as we are aware, the second novelty lies in the gene therapy approach delivered by IVT injection. Although AAV2 IVT-based gene therapies are already in clinical trials for retinal ganglion cell diseases, our approach targets photoreceptors by delivering an engineered cDNA construct that releases the extracellular therapeutic agent directly into the retinal environment. This method avoids the risks associated with retinal detachment and offers broad retinal coverage, unlike the localized distribution achieved with subretinal injections.

The multifunctionality of the full-length PEDF protein arises from a complex interaction among its bioactive domains and multiple receptors[53,54]. In this context, peptide fragmentation is particularly valuable for isolating the distinct actions of PEDF. A substantial body of research on PEDF peptide fragments supports their therapeutic potential, although many studies have focused on non-ocular applications[23,55–58]. Limited yet promising research has investigated the topical application of PEDF-derived peptides in the eye[59]. For instance, the 17-mer peptide demonstrated partial photoreceptor protection in MITF mice, suggesting its potential for retinal preservation through eye drops (33). In models of diabetic retinopathy, the 44-mer peptide penetrated the cornea and reduced retinal inflammation, underscoring its neuroprotective properties[60]. The 44-mer and 29-mer peptides have also shown anti-inflammatory effects in murine models of corneal injury and dry eye[61,62]. Meanwhile, peptides derived from the anti-angiogenic region of PEDF (34-mer), distinct from the neurotrophic 44-mer region, effectively reduced experimental choroidal and retinal neovascularization in mice and rabbits when administered via IVT injection, either alone, with collagen, or encapsulated in nanoparticles[23,55,63,64]. It is crucial to note that the 17-mer peptide does not bind antiangiogenic receptors such as the laminin receptor, ATPase, and LPR6, instead, this region is specifically neurotrophic, binding to PEDF-R and making other receptor interactions less relevant to our study[23,29,53]. This specific receptor binding profile highlights the therapeutic potential of the 17-mer peptide in targeting neuroprotection without activating antiangiogenic pathways.

We also acknowledge uncertainties regarding i) the extent to which ocular penetration in animal models translates into humans, ii) the durability of the therapeutic effects, iii) prior evidence supporting topical delivery of PEDF-derived peptides for neuroprotection, and iv) the relative benefits and drawbacks of IVT versus subretinal gene therapy delivery. Notably, the AAV2 subretinal delivery has been approved for delivering RPE65[65,66]. However, in our study, IVT injection was preferred as transducing photoreceptor cells was unnecessary. PEDF exerts its effects through paracrine signaling, where it is secreted by supporting tissues, like the RPE and Müller cells, to act on photoreceptors, rather than autocrine pathways[16,23]. Additionally, the IVT route enables a uniform distribution of H105A-expressing cells across the retina, avoiding retinal detachment and other side effects associated with subretinal injections.

Although PEDF peptides 17-mer and H105A show promise in preclinical studies, further research is essential to optimize their delivery methods and establish their long-term safety and efficacy. Nevertheless, our findings advance the understanding of how the structure-activity relationships of naturally occurring bioactive proteins can facilitate therapeutic drug development.

In conclusion, we present compounds and methods for treating retinal degeneration using PEDF-derived peptides. This modality of peptide therapeutics is promising for photoreceptor death prevention in several retinopathies, and the topical ocular peptide delivery has potential for translation into safer, less-invasive applications to stabilize and delay the progression of neurodegeneration in retinal disorders, particularly in a large proportion of RP patients.

Data availability

All data are available in the main text or the supplementary materials. The source data and statistical analysis for all figures are accessible from the Supplementary Data 1 file. Any additional information required to reanalyze the data reported in this paper is available from the corresponding authors upon request.

Received: 26 June 2024; Accepted: 27 February 2025;
Published online: 21 March 2025

References

1. Hartong, D. T., Berson, E. L. & Dryja, T. P. Retinitis pigmentosa. *Lancet* **368**, 1795–1809 (2006).
2. T. B. O'Neal, E. E. Luther, in *StatPearls*. (Treasure Island (FL), 2024).
3. Hanany, M., Rivolta, C. & Sharon, D. Worldwide carrier frequency and genetic prevalence of autosomal recessive inherited retinal diseases. *Proc. Natl. Acad. Sci. USA* **117**, 2710–2716 (2020).
4. Chew, L. A. & Iannaccone, A. Gene-agnostic approaches to treating inherited retinal degenerations. *Front. Cell Dev. Biol.* **11**, 1177838 (2023).
5. Kutluer, M., Huang, L. & Marigo, V. Targeting molecular pathways for the treatment of inherited retinal degeneration. *Neural Regen. Res.* **15**, 1784–1791 (2020).
6. Hejtmancik, J. F. & Daiger, S. P. Understanding the genetic architecture of human retinal degenerations. *Proc. Natl Acad. Sci. USA* **117**, 3904–3906 (2020).
7. Roska, B. & Sahel, J. A. Restoring vision. *Nature* **557**, 359–367 (2018).
8. Sahel, J. A., Bennett, J. & Roska, B. Depicting brighter possibilities for treating blindness. *Sci. Transl. Med.* **11**, eaax2324 (2019).
9. Himawan, E. et al. Drug delivery to retinal photoreceptors. *Drug Discov. Today* **24**, 1637–1643 (2019).
10. Rowe-Rendleman, C. L. et al. Drug and gene delivery to the back of the eye: from bench to bedside. *Invest Ophthalmol. Vis. Sci.* **55**, 2714–2730 (2014).
11. Gabai, A., Zeppieri, M., Finocchio, L. & Salati, C. Innovative Strategies for Drug Delivery to the Ocular Posterior Segment. *Pharmaceutics* **15**, 1862 (2023).
12. Chang, B. et al. Retinal degeneration mutants in the mouse. *Vis. Res* **42**, 517–525 (2002).
13. Arango-Gonzalez, B. et al. Identification of a common non-apoptotic cell death mechanism in hereditary retinal degeneration. *PLoS One* **9**, e112142 (2014).
14. Gargini, C., Terzibasi, E., Mazzoni, F. & Strettoi, E. Retinal organization in the retinal degeneration 10 (rd10) mutant mouse: a morphological and ERG study. *J. Comp. Neurol.* **500**, 222–238 (2007).
15. Barhoum, R. et al. Functional and structural modifications during retinal degeneration in the rd10 mouse. *Neuroscience* **155**, 698–713 (2008).
16. Dixit, S. et al. PEDF deficiency increases the susceptibility of rd10 mice to retinal degeneration. *Exp. Eye Res* **198**, 108121 (2020).
17. Sakami, S. et al. Probing mechanisms of photoreceptor degeneration in a new mouse model of the common form of autosomal dominant retinitis pigmentosa due to P23H opsin mutations. *J. Biol. Chem.* **286**, 10551–10567 (2011).
18. Bighinati, A., Adani, E., Stanzani, A., D'Alessandro, S. & Marigo, V. Molecular mechanisms underlying inherited photoreceptor degeneration as targets for therapeutic intervention. *Front Cell Neurosci.* **18**, 1343544 (2024).
19. Murakami, Y., Nakabeppu, Y. & Sonoda, K. H., Oxidative Stress and Microglial Response in Retinitis Pigmentosa. *Int. J. Mol. Sci.* **21**, 7170 (2020).
20. Kutsyr, O. et al. Short-term high-fat feeding exacerbates degeneration in retinitis pigmentosa by promoting retinal oxidative stress and inflammation. *Proc. Natl. Acad. Sci. USA* **118**, e2100566118 (2021).

21. Gallenga, C. E. et al. Molecular Mechanisms Related to Oxidative Stress in Retinitis Pigmentosa. *Antioxidants (Basel)* **10**, (2021).
22. Polato, F. & Becerra, S. P. Pigment Epithelium-Derived Factor, a Protective Factor for Photoreceptors in Vivo. *Adv. Exp. Med Biol.* **854**, 699–706 (2016).
23. Rebustini, I. T., Bernardo-Colon, A., Nalvarte, A. I. & Becerra, S. P. Delivery Systems of Retinoprotective Proteins in the Retina. *Int. J. Mol. Sci.* **22**, 5344 (2021).
24. Rasmussen, H. et al. Clinical protocol. An open-label, phase I, single administration, dose-escalation study of ADGVPEDF.11D (ADPEDF) in neovascular age-related macular degeneration (AMD). *Hum. Gene Ther.* **12**, 2029–2032 (2001).
25. Pagan-Mercado, G. & Becerra, S. P. Signaling Mechanisms Involved in PEDF-Mediated Retinoprotection. *Adv. Exp. Med Biol.* **1185**, 445–449 (2019).
26. Notari, L. et al. Identification of a lipase-linked cell membrane receptor for pigment epithelium-derived factor. *J. Biol. Chem.* **281**, 38022–38037 (2006).
27. Subramanian, P. et al. Pigment epithelium-derived factor (PEDF) prevents retinal cell death via PEDF Receptor (PEDF-R): identification of a functional ligand binding site. *J. Biol. Chem.* **288**, 23928–23942 (2013).
28. Bernardo-Colon, A. et al. Ablation of pigment epithelium-derived factor receptor (PEDF-R/Pnpla2) causes photoreceptor degeneration. *J. Lipid Res* **64**, 100358 (2023).
29. Kenealey, J. et al. Small Retinoprotective Peptides Reveal a Receptor-binding Region on Pigment Epithelium-derived Factor. *J. Biol. Chem.* **290**, 25241–25253 (2015).
30. Comitato, A. et al. Pigment epithelium-derived factor hinders photoreceptor cell death by reducing intracellular calcium in the degenerating retina. *Cell Death Dis.* **9**, 560 (2018).
31. Hernandez-Pinto, A. et al. PEDF peptides promote photoreceptor survival in rd10 retina models. *Exp. Eye Res.* **184**, 24–29 (2019).
32. Valiente-Soriano, F. J. et al. Pigment Epithelium-Derived Factor (PEDF) Fragments Prevent Mouse Cone Photoreceptor Cell Loss Induced by Focal Phototoxicity In Vivo. *Int. J. Mol. Sci.* **21**, 7242 (2020).
33. Chen, Y. et al. Photoreceptor degeneration in microphthalmia (Mitf) mice: partial rescue by pigment epithelium-derived factor. *Dis. Model Mech.* **12**, dmm035642 (2019).
34. Yao, D. et al. Enhancing soluble expression of sucrose phosphorylase in Escherichia coli by molecular chaperones. *Protein Expr. Purif.* **169**, 105571 (2020).
35. Wang, X., Li, J., Lin, X. & Zhang, Y. The s-oph enzyme for efficient degradation of polyvinyl alcohol: soluble expression and catalytic properties. *Mol. Biol. Rep.* **50**, 8523–8535 (2023).
36. Mazzoni, F. et al. Non-invasive in vivo fluorescence imaging of apoptotic retinal photoreceptors. *Sci. Rep.* **9**, 1590 (2019).
37. Maidana, D. E. et al. A Novel ImageJ Macro for Automated Cell Death Quantitation in the Retina. *Invest. Ophthalmol. Vis. Sci.* **56**, 6701–6708 (2015).
38. Jouanneau, J. et al. Secreted or nonsecreted forms of acidic fibroblast growth factor produced by transfected epithelial cells influence cell morphology, motility, and invasive potential. *Proc. Natl Acad. Sci. USA* **88**, 2893–2897 (1991).
39. Allocca, M. et al. Novel adeno-associated virus serotypes efficiently transduce murine photoreceptors. *J. Virol.* **81**, 11372–11380 (2007).
40. Della Santina, L. et al. Processing of retinal signals in normal and HCN deficient mice. *PLoS One* **7**, e29812 (2012).
41. Zhong, X. et al. Generation of three-dimensional retinal tissue with functional photoreceptors from human iPSCs. *Nat. Commun.* **5**, 4047 (2014).
42. Vergara, M. N. et al. Three-dimensional automated reporter quantification (3D-ARQ) technology enables quantitative screening in retinal organoids. *Development* **144**, 3698–3705 (2017).
43. Nagata, S., Suzuki, J., Segawa, K. & Fujii, T. Exposure of phosphatidylserine on the cell surface. *Cell Death Differ.* **23**, 952–961 (2016).
44. Murakami, Y. et al. Inhibition of nuclear translocation of apoptosis-inducing factor is an essential mechanism of the neuroprotective activity of pigment epithelium-derived factor in a rat model of retinal degeneration. *Am. J. Pathol.* **173**, 1326–1338 (2008).
45. Comitato, A., Schiroli, D., Montanari, M. & Marigo, V. Calpain Activation Is the Major Cause of Cell Death in Photoreceptors Expressing a Rhodopsin Misfolding Mutation. *Mol. Neurobiol.* **57**, 589–599 (2020).
46. Koponen, S., Kokki, E., Tamminen, T. & Ylä-Herttuala, S. AAV2 and AAV9 tropism and transgene expression in the mouse eye and major tissues after intravitreal and subretinal delivery. *Front. Drug Deliv.* **3**, 1148795 (2023).
47. Onyak, J. R., Vergara, M. N. & Renna, J. M. Retinal organoid light responsivity: current status and future opportunities. *Transl. Res.* **250**, 98–111 (2022).
48. Bertram, K. M., Baglole, C. J., Phipps, R. P. & Libby, R. T. Molecular regulation of cigarette smoke induced-oxidative stress in human retinal pigment epithelial cells: implications for age-related macular degeneration. *Am. J. Physiol. Cell Physiol.* **297**, C1200–C1210 (2009).
49. Yu, A. L., Birke, K., Burger, J. & Welge-Lussen, U. Biological effects of cigarette smoke in cultured human retinal pigment epithelial cells. *PLoS One* **7**, e48501 (2012).
50. Henning, Y. et al. Cigarette smoke causes a bioenergetic crisis in RPE cells involving the downregulation of HIF-1alpha under normoxia. *Cell Death Discov.* **9**, 398 (2023).
51. Sidman, R. L. et al. The peptidomimetic Vasotide targets two retinal VEGF receptors and reduces pathological angiogenesis in murine and nonhuman primate models of retinal disease. *Sci. Transl. Med.* **7**, 309ra165 (2015).
52. Falsini, B. et al. NGF eye-drops topical administration in patients with retinitis pigmentosa, a pilot study. *J. Transl. Med* **14**, 8 (2016).
53. Xu, M. M., Chen, X., Yu, Z. & Li, X. Receptors that bind to PEDF and their therapeutic roles in retinal diseases. *Front. Endocrinol.* **14**,1116136. (2023).
54. Crawford, S. E., Fitchev, P., Veliceasa, D. & Volpert, O. V. The many facets of PEDF in drug discovery and disease: a diamond in the rough or split personality disorder? *Expert Opin. Drug Discov.* **8**, 769–792 (2013).
55. Qu, Q. et al. Sustained therapeutic effect of an anti-inflammatory peptide encapsulated in nanoparticles on ocular vascular leakage in diabetic retinopathy. *Front Cell Dev. Biol.* **10**, 1049678 (2022).
56. Tombran-Tink, J. PEDF in angiogenic eye diseases. *Curr. Mol. Med.* **10**, 267–278 (2010).
57. Elmi, M., Dass, J. H. & Dass, C. R. The Various Roles of PEDF in Cancer. *Cancers* **6**, 510 (2014).
58. Ek, E. T., Dass, C. R. & Choong, P. F. Pigment epithelium-derived factor: a multimodal tumor inhibitor. *Mol. Cancer Ther.* **5**, 641–646 (2016).
59. Sun, M. H., Ho, T. C., Yeh, S. I., Chen, S. L. & Tsao, Y. P. Short peptides derived from pigment epithelium-derived factor attenuate retinal ischemia reperfusion injury through inhibition of apoptosis and inflammatory response in rats. *Exp. Eye Res.* **238**, 109743 (2024).
60. Liu, Y. et al. Pigment epithelium-derived factor (PEDF) peptide eye drops reduce inflammation, cell death and vascular leakage in diabetic retinopathy in Ins2(Akita) mice. *Mol. Med.* **18**, 1387–1401 (2012).
61. Yeh, S. I. et al. Pigment Epithelial-Derived Factor Peptide Facilitates the Regeneration of a Functional Limbus in Rabbit Partial Limbal Deficiency. *Invest Ophthalmol. Vis. Sci.* **56**, 2126–2134 (2015).
62. Ho, C., Fan, N. W., Yeh, S. I., Chen, S. L. & Tsao, Y. P. The Therapeutic Effects of a PEDF-Derived Short Peptide on Murine Experimental Dry Eye Involves Suppression of MMP-9 and Inflammation. *Transl. Vis. Sci. Technol.* **11**, 12 (2022).

63. Amaral, J. & Becerra, S. P. Effects of human recombinant PEDF protein and PEDF-derived peptide 34-mer on choroidal neovascularization. *Invest Ophthalmol. Vis. Sci.* **51**, 1318–1326 (2010).
64. Sheibani, N. et al. Inhibition of retinal neovascularization by a PEDF-derived nonapeptide in newborn mice subjected to oxygen-induced ischemic retinopathy. *Exp. Eye Res.* **195**, 108030 (2020).
65. Maguire, A. M. et al. Safety and efficacy of gene transfer for Leber's congenital amaurosis. *N. Engl. J. Med.* **358**, 2240 (2008).
66. Bainbridge, J. W. B. et al. Effect of gene therapy on visual function in Leber's congenital amaurosis. *N. Engl. J. Med.* **358**, 2231 (2008).

Acknowledgements

We thank Megan Kopera for assistance with animal husbandry, Haohua Qian for assistance and usage of the Visual Function Core, Maria Campos for service of the Histology Core and Robert Fariss for access to the NEI bioimaging Core. We thank K. Palczewski for the *Rho*$^{P23H/+}$ mouse model. We thank K. Bharti for proofreading this manuscript. This work was supported by the Intramural Research Program of the National Eye Institute, National Institutes of Health, United States of America (Project #EY000306, SPB); the Prevention of Blindness Society (SPB); Fondazione Telethon (Project #GGP19113, VM), the National Center for "Gene Therapy and Drugs based on RNA Technology" cod. Progetto CN00000041 and "Health Extended Alliance for Innovative Therapies, Advanced Lab-research, and Integrated Approaches of Precision Medicine - HEAL ITALIA" tematica 6 "Innovative diagnostics and therapies in precision medicine" cod. Progetto PE0000019 PIANO NAZIONALE DI RIPRESA E RESILIENZA (PNRR) – MISSIONE 4 "Istruzione Ricerca" COMPONENTE 2, "Dalla ricerca all'impresa" INVESTIMENTO 1.4, "Potenziamento strutture di ricerca e creazione di "campioni nazionali di R&S" su alcune Key enabling technologies", finanziato dall'Unione europea – NextGenerationEU (VM and AB); The CellSight Development Fund (NV); and a Challenge Grant to the Department of Ophthalmology at the University of Colorado from Research to Prevent Blindness (NV).

Author contributions

A.B.C. contributed Methodology, Investigation, Formal analysis, Visualization, Writing - original draft, Writing - review & editing. A.B. contributed Investigation, Formal analysis, Visualization, Writing - review & editing. S.P. contributed Investigation, Formal analysis, Visualization, Writing - review & editing. S.D. contributed Investigation, Visualization, Writing - review & editing. I.P contributed Formal analysis, Writing - review & editing. E.A. contributed Investigation. F.C. contributed Investigation. C.G. contributed Formal analysis, Writing - review & editing. N.V. contributed Conceptualization, Methodology, Visualization, Funding acquisition, Supervision, Writing - review & editing. V.M. contributed Conceptualization, Methodology, Funding acquisition, Supervision, Writing - review & editing. S.P.B. contributed Conceptualization, Methodology, Visualization, Funding acquisition, Project administration, Supervision, Writing - review & editing.

Funding

Open access funding provided by the National Institutes of Health.

Competing interests

US Government and University of Modena and Reggio Emilia, Italy. S. P. Becerra, A. Bernardo-Colón, V. Marigo, A Bighinati. US Application No. 63 430 251 NIH Ref No E-028-2023-0-US-01 and international application PCT/US2023/064947, filed on March 24, 2023. The specific aspect of the manuscript covered in the patent applications is on PIGMENT EPITHELIUM-DERIVED FACTOR PEPTIDES AND USE FOR TREATING RETINAL DEGENERATION.

Additional information

Supplementary information The online version contains supplementary material available at https://doi.org/10.1038/s43856-025-00789-8.

Correspondence and requests for materials should be addressed to Valeria Marigo or S. Patricia Becerra.

Peer review information *Communications Medicine* thanks Thomas Corydon and the other, anonymous, reviewer(s) for their contribution to the peer review of this work.